Reevaluation of Thermodynamic Models for Phase Diagram Evaluation

By H. Okamoto
ASM International
Materials Park, OH 44073

Several thermodynamic models for calculating binary phase diagrams published in the literature have been reevaluated. Problems in some of these models are already evident in the models themselves and may also be seen in the resulting calculated phase diagrams. When a calculation is attempted, thermodynamic models with quite different formulations may result in very similar proposed phase diagrams. In such cases, if experimental data of a binary phase diagram can be represented reasonably well by several different thermodynamic models, a simpler model often provides the clearest insight into the basic properties of the system. If a calculated phase diagram results in unusual phase relationships, the adopted thermodynamic model may be inappropriate or may involve unrealistic parameters. If the thermodynamic model is clearly unrealistic and yet the calculated phase diagram appears to be normal, errors in calculation or in interpretation may be suspect. Various examples of unlikely combinations of thermodynamic models and phase diagrams are discussed.

1. Introduction

During editing of the graphics for the compilation of the binary phase diagrams published in [90Mas], many diagrams were recognized as showing features that would be very difficult or impossible to reconcile (*i.e.*, to model) thermodynamically. In most cases, only minor changes were sufficient to save the thermodynamic integrity of the proposed diagram, and usually it was modified accordingly. [91Oka] summarized some typical examples of the encountered problems, which were occasionally found even in otherwise carefully assessed phase diagrams. However, another group of phase diagrams and assessments with potential problems were not corrected, or questioned in [90Mas]. These calculated diagrams did not appear to be violating any phase rules, but could nevertheless be considered to have been derived from unusual thermodynamic models. Some of these diagrams are the subject of the present paper.

Thermodynamic calculations of phase diagrams recently became easier to perform because of the development of standard computer programs based on the pioneering works of [70Kau], [77Luk], and [82Pel]. These programs permit the derivation of thermodynamic functions of relevant phases by optimizing the input data on some available measured thermodynamic properties of such phases and also by utilizing experimentally derived portions of the phase diagram of a given system. Because the resulting calculated diagram may appear to represent the experimental data quite adequately, insufficient attention may be paid to the actual thermodynamic functions developed and utilized in the calculation. As a result, it is not rare to find thermodynamic models that involve functions with parameters of hardly credible magnitude. Such functions would be particularly inappropriate if they were subsequently used for purposes other than phase diagram modeling, for example if they were made the basis of predicting metastable situations, or used in kinetic calculations.

This article aims to emphasize that quite simple thermodynamic models are often nevertheless more informative than those with very sophisticated formulation. The basic validity of a simple model is generally more easy to examine with regard to the thermodynamic and physical properties associated with a given binary system. In most situations of the present work, the temperature dependence of the specific heats of all phases is assumed to be equal, *i.e.*, $\Delta C_p = 0$. This approach may appear to be opposite to the trend of current interest on formation of a metastable crystalline phase or an amorphous phase by nonequilibrium reactions at low temperatures [86Sau, 88Bor, 89Pam, 91Fec]. In such a case, the temperature dependence of ΔC_p of the individual phase has an important meaning, and interesting problems such as Kauzmann's paradox [48Kau, 88Fec] or inverse melting [88Gre] may arise. However, the present discussion deals with situations of equilibrium phase transformations at high temperatures where the specific heat of relevant phases usually varies slowly with temperature. In this range, the temperature dependence of ΔC_p is not a major concern, especially in phase diagram calculation. The present discussion is also limited mostly to binary systems with well-behaved properties, *e.g.*, systems that tend not to form associations in the liquid state. This is not atypical, however, because most metal-metal systems fall into this category.

2. Basic Principles of Thermodynamic Calculation

A few fundamental principles of thermodynamic modeling of phase diagrams are reviewed in this section in order to introduce terminologies and mathematical expressions that are used in later sectionss. Various standard references, such as [56Rhi] and [68Gor], provide more detailed information on thermodynamic modeling.

Figure 1(a) shows a simple phase diagram of a system *A-B* with a completely miscible liquid phase, L, and a solid phase of the component (*A*) having no solid solubility of the second component, *B*.

Figure 1(b) shows the corresponding Gibbs energy diagram at $T = T_1$. The composition b of the liquid in equilibrium with (A) at T_1 can be obtained by drawing a straight line from the point a, which represents the Gibbs energy of the solid A at temperature T_1, to the Gibbs energy curve of the liquid phase, $\Delta_{mix}G(L)$, so that the line is tangential to the curve. As is well known, this corresponds to the situation of the minimum total free energy for the solid + liquid mixture of the two phases in the binary system. In this diagram, the zero points (reference states) of the Gibbs energies for elements A and B are liquid A and liquid B, respectively. The position of the point a, with respect to the zero point as a function of temperature, is referred to as the lattice stability parameter, $G^0(A)$, of the element A. Here, the superscript zero on G stands for the standard pressure, *i.e.*, 1 atm. The Gibbs energy curve, $\Delta_{mix}G(L)$, represents the change of the Gibbs energy (free energy under a constant pressure) gained by forming a liquid alloy from pure liquid A and pure liquid B and is expressed by

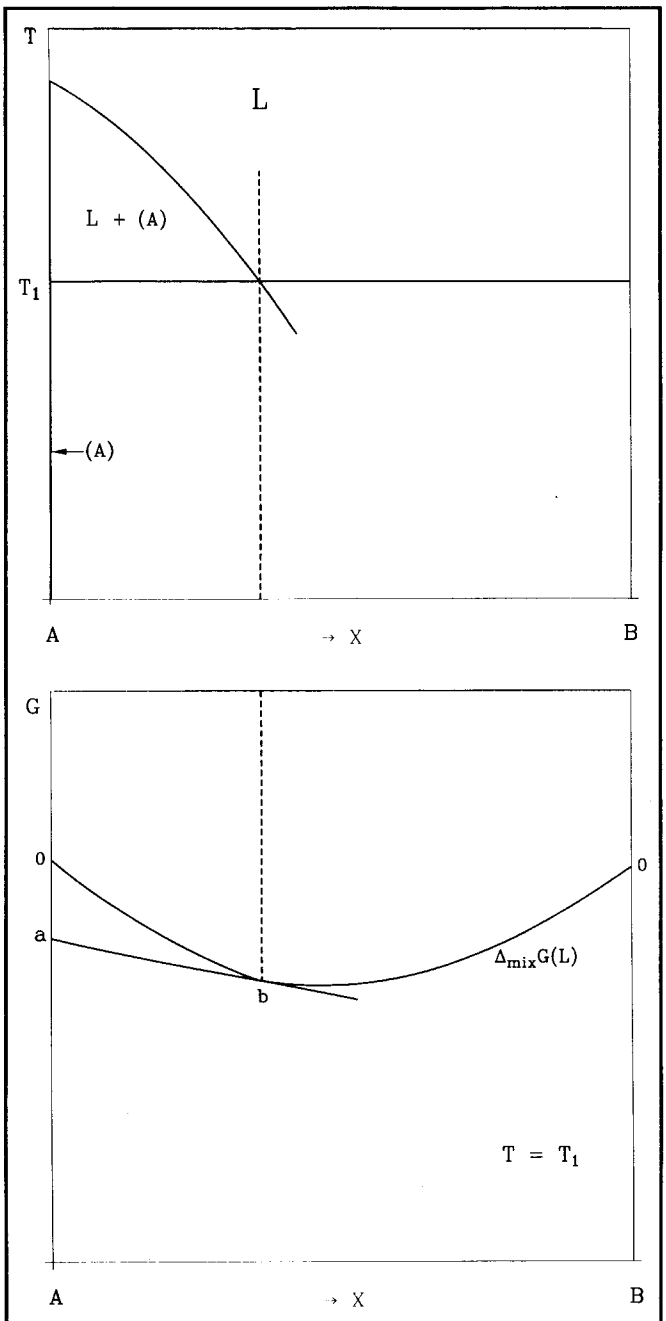

Fig. 1 (a) *A-B* phase diagram. The liquid phase is completely miscible and the (A) phase has no solid solubility range. **(b)** Gibbs energy diagram at $T = T_1$. Point a represents lattice stability parameter of A. The line ab is drawn to contact the Gibbs energy of mixing curve, $\Delta_{mix}G(L)$, of the liquid phase. The point of contact b shows the liquidus composition.

$$\Delta_{mix}G(L) = RT[X\ln X + (1-X)\ln(1-X)] + \Delta_{mix}G^{ex}(L)$$

where X is the atomic fraction of the element B in the mixture*. The first term represents the energy lowering due to the ideal mixing of A and B (*i.e.*, the entropy related term), and the second term represents the excess quantity (*i.e.*, contributions due to deviation from ideal mixing caused by interaction between A and B). The liquid is an ideal solution when $\Delta_{mix}G^{ex}(L) = 0$

$\Delta_{mix}G^{ex}(L)$, which is in principle a function of both composition X and temperature T (K), consists of an enthalpy term** and an excess entropy term:

$$\Delta_{mix}G^{ex}(L) = \Delta_{mix}H(L) - T\Delta_{mix}S^{ex}(L)$$

In this article, $\Delta_{mix}G^{ex}(L)$ is also often expressed as

$$\Delta_{mix}G^{ex}(L) = X(1-X)[h(L) - Ts(L)]$$

The parabolic function $X(1-X)$ is the consequence of near neighbor interaction statistics and it expresses the fact that both $\Delta_{mix}H(L)$ (or $X(1-X)h(L)$) and $\Delta_{mix}S^{ex}(L)$ (or $X(1-X)s(L)$) must always be 0 at $X = 0$ and $X = 1$. Generally, the h and s parameters*** are composition and temperature dependent. Also, the h and s functions are not completely independent, because the enthalpy and entropy of mixing, $\Delta_{mix}H(L)$ and $\Delta_{mix}S^{ex}(L)$, themselves derive from the same quantity $\Delta_{mix}C_p(L)$ (specific heat of mixing) through the expressions

$$\Delta_{mix}H(L) = \int \Delta_{mix}C_p(L)\, dT$$

and

$$\Delta_{mix}S^{ex}(L) = \int \Delta_{mix}C_p(L)/T\, dT$$

as discussed in more detail in subsection 4.3. When $\Delta_{mix}C_p(L)$ is zero, the h and s functions do not include temperature terms (consisting of integration constants only, which may be composition dependent). When $s = 0$ and h is fixed (composition independent), the solution is called a regular solution. When $s = 0$ and h changes with composition, the solution is subregular. For simplicity, the composition dependence of h in this article (except in section 4) is expressed as a power function of X

$$h = h_0 + h_1X + h_2X^2 + ... + h_nX^n$$

* Throughout this article, X is used as the atomic fraction of the element on the right-hand side of the phase diagram.

** The enthalpy of mixing is always an excess quantity because it is zero for an ideal solution.

*** The designation of the phase, (L) in this case, is omitted when no confusion arises through the omission. All expressions for the L phase are also applicable to any other phase. The h and s are sometimes called interaction parameters.

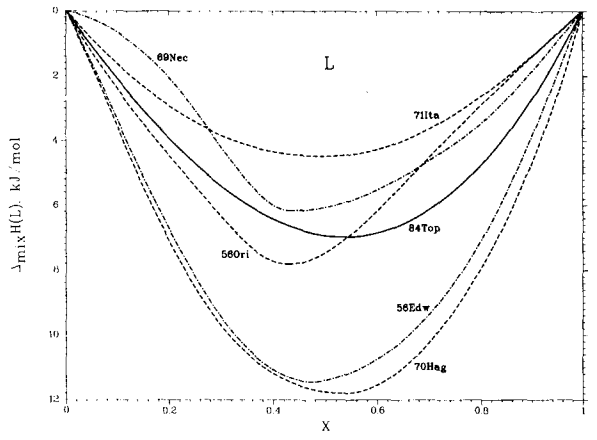

Fig. 2 Enthalpy of mixing of the Au-Cu liquid alloys reported by various investigators. From [87Oka1].

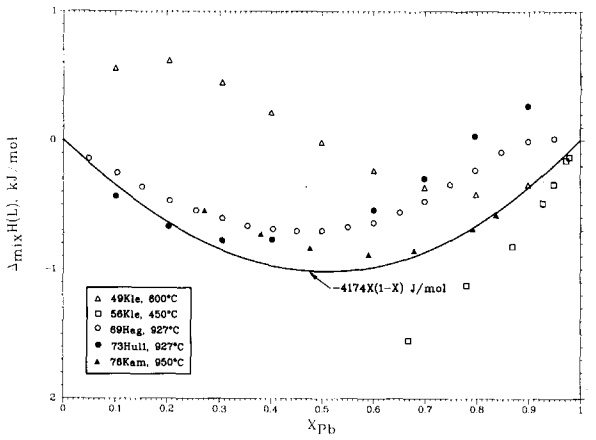

Fig. 3 Enthalpy of mixing of the Au-Pb liquid alloys reported by various investigators. From [84Oka2].

rather than the Redlich-Kister or the Legendre polynomial expressions (often used in the literature). Similarly,

$$s = s_0 + s_1X + s_2X_2 + ... + s_nX^n$$

In principle, h_i and s_i can be temperature dependent and also related to one another via the specific heat term, as already mentioned.

Of course, most phase diagrams are more complex than that shown in Fig. 1(a). They frequently involve appreciable solid solubility ranges and numerous intermediate phases or compounds. [87Oka2] summarized some hints for thermodynamic modeling and calculation for such situations.

3. Reliability of Thermodynamic Data

This section emphasizes that experimental thermodynamic data available in the literature are generally not very reliable. Accordingly, it may not be always worthwhile to try to develop a thermodynamic model that would closely represent all the reported experimental thermodynamic data.

For example, one might expect that the enthalpy of mixing of the Au-Cu liquidus is by now well determined, because the noble metals Au and Cu are not strongly reactive with most environmental elements (*i.e.*, impurity problems should be of minor importance) and their melting temperatures are similar. However, the experimental data are far from unanimous. Figure 2 (from [87Oka1]) shows the composition dependence of enthalpy of mixing of the Au-Cu liquid alloys reported by various investigators. According to the most recent measurement by [84Top], the enthalpy of mixing trend shows a well-behaved, nearly parabolic form. If a thermodynamic modeling had been attempted before 1984, the enthalpy of mixing could have been assumed to be: twice as large in magnitude, based on [56Edw] and [70Hag]; or only about 2/3 as large, based on [71Ita]; or even having a marked composition dependence, based on [56Ori] or [69Nec]. Perhaps surprisingly, the consequence of such differences may nevertheless turn out not to be serious in calculation of the equilibrium phase diagrams, as shown in a later discussion. For example, in spite of substantial differences in the magnitudes of the enthalpy of mixing, all data shown in Fig. 2 are within tolerable limits when compared with gigantic deviations that are evident in some models referred to below.

The enthalpy of mixing of the Au-Pb liquid alloys, shown in Fig. 3 [84Oka2], provides another example. Because the enthalpy of mixing values, measured by [49Kle], [56Kle], [69Hag], and [76Kam] at different temperatures, differ significantly, it could be assumed that the temperature dependence of the enthalpy of mixing is substantial and should be accounted for via a suitable expression. However, the appearance of the temperature dependence is far too complex, and modeling using only a limited number of parameters is not possible. Fortunately, in most such cases the temperature dependence of the enthalpy and of the excess entropy of mixing can be assumed to be rather small, or zero, at least at higher temperatures. (If they are not zero, the specific heat of mixing would have to be considered. See subsection 4.3.) Most likely, much, if not all, of the measured data in Fig. 3 are not particularly accurate.

If, however, only one set of thermodynamic data is known for a particular system under study, there may be a temptation to develop a model that represents that specific data as closely as possible, including both the temperature and composition dependence. However, as mentioned above, such an effort may be unfounded because there is no guarantee that the particular set of data is correct.

These comments emphasize that thermodynamic data, such as the enthalpy of mixing, must be used with caution if they are to be utilized as the primary source of information for a phase diagram calculation, unless firmly established by several independent investigations. More appropriately, the literature data mainly serve as guidelines for the likely magnitudes involved. As shown later, a moderately inappropriate selection of thermodynamic functions may not necessarily cause a serious problem in an attempt to reproduce the correct features of a given phase diagram.

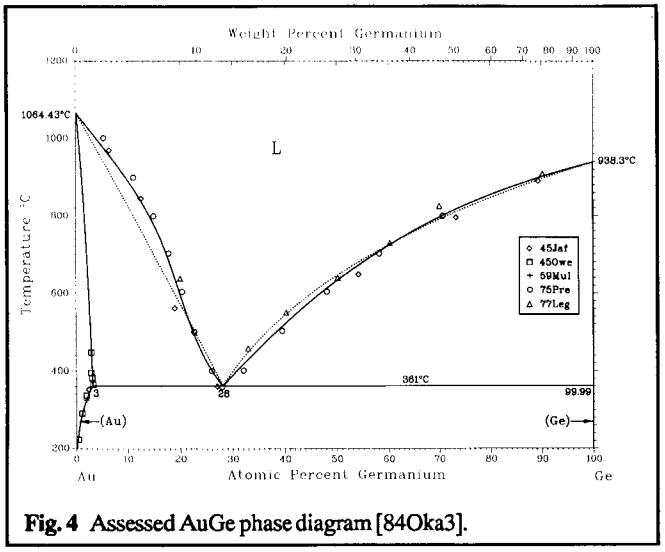

Fig. 4 Assessed AuGe phase diagram [84Oka3].

4. Simplification of Thermodynamic Models

This section illustrates that a simpler thermodynamic model often is more informative and meaningful in reference to a calculated phase diagram when compared with models adopting more complex thermodynamic formulations. Quite often, when thermodynamic data are not available, a model that neglects the excess entropy of mixing term nevertheless serves quite well.

4.1 Selection of the Lattice Stability Parameters

The lattice stability parameter G^0(s) of a certain lattice structure in the solid state (s) of an element A, with respect to the liquid state, is commonly expressed as

$$G^0(s) = \int \Delta C_p\, dT - T\int \Delta C_p/T\, dT \qquad \text{Eq 1}$$

where ΔC_p is the difference between specific heats of s and L. In principle, specific heat (C_p) of s or L can be measured accurately in the temperature range where the given phase is stable. Although the data on the C_p of a solid is usually available accurately below the melting point, the C_p of the corresponding liquid is rarely available in the same temperature range because it would require measurements in an undercooled liquid. Therefore, ΔC_p can rarely be determined with needed accuracy. In many thermodynamic models, the temperature dependence of the C_p of s is derived directly from experimental data observed below the melting point, and the C_p of L is assumed to be constant, or behaving as an extrapolation from the data above the melting point. In general, the lattice stability parameters obtained in this way are applied for both above and below the melting point. The validity of this assumption cannot be confirmed experimentally, except for a rather narrow undercooling range in some specific systems.

An attempt to calculate the phase equilibria in the Au-Ge system [84Oka3] may be used as an illustration of the point that an assumption of $\Delta C_p = 0$ may sufficiently represent the experimental data for the equilibrium liquidus. The entire Au-Ge phase diagram (Fig. 4) was actually calculated in [84Oka3], but here only the L/[L + (Ge)] liquidus is discussed. The relevant thermodynamic functions adopted in [84Oka3] are:

$$G^0(\text{Ge,diamond}) = -34\,006 - 10.954T + 6T\ln T - 0.00295T^2 \text{ J/mol} \qquad \text{Eq 2}$$

for the lattice stability parameter* of the solid Ge phase and

$$\Delta_{mix}G^{ex}(L) = X(1-X)[-3300 + 25\,900X - (23.91 - 58.16X + 54.13X^2)T] \text{ J/mol}$$

for the Gibbs energy of mixing of the liquid phase. Equation 2 was derived by substituting $\Delta C_p = 5.9 \times 10^{-3}T - 6$ J/mol into Eq 1, where the specific heat data for the solid phase were adopted from [77Bar] and the constant value of the specific heat for the liquid phase was also obtained from [77Bar], assuming that C_p(L) above the melting point of Ge (938.3 °C) is applicable to a reasonably wide interval of T below the melting point.

A much simpler lattice stability parameter

$$G^0(\text{Ge,diamond}) = -37\,030 + 30.567T \text{ J/mol} \qquad \text{Eq 3}$$

can be derived from the enthalpy of fusion data given in [83Cha] and the melting point of Ge, together with the assumption of $\Delta C_p = 0$. The liquidus boundary calculated with this lattice stability parameter, Eq 3, and the excess Gibbs energy of

$$\Delta_{mix}G^{ex}(L) = X(1-X)(-26\,126 + 8988X) \text{ J/mol}$$

is nearly identical (no essential difference is seen on a diagram of ordinary scale) with the assessed boundary obtained by using the lattice stability parameter as given in Eq 2. The simpler representation of the latter involves only two parameters each for the lattice stability parameter and the Gibbs energy of mixing, whereas the former involves four and five parameters, respectively. Because the calculated results are almost identical and the superiority of one model over the other is unknown, the simpler model may be preferable if an attempt is made to comprehend the general thermodynamic properties of the system and avoid errors. For example, the temperature dependence of G^0(Ge,diamond) in Eq 2 is difficult to visualize. Even if there were any problem in this model, *e.g.*, if the expression were unrealistic, involving a wrong melting point, or an anomalous temperature dependence, or if there was a typing error, the problem would be unnoticed until a phase diagram calculation was attempted. On the other hand, Eq 3 is much easier to comprehend and less prone to errors. (The constant term is the enthalpy of fusion, which must be equal to the product of the coefficient of the linear term and the melting point in K.) Figure 5 shows the difference in the temperature dependence of the respective lattice stability parameters. It can be seen that the complex expression of Eq 2 does not differ much from the simple expression of Eq 3.

*Unless specified otherwise, the reference states of lattice stability parameters and Gibbs energies of formation of compounds are liquid elements throughtout this article. The temperature dependence of Eq 2 is derived from ΔC_p having a linear temperature dependence. By writing C_p as $a + bT$, $G = \int(a + bT)\,dT - T\int(a/T + b)dT = (aT + \frac{1}{2}bT^2 + K_1) - T(a\ln T + bt + K_2) = K_1 + (a - K_2)T - aT\ln T - \frac{1}{2}bT^2$ according to Eq 1. Integral constants K_1 and K_2 are usually determined from the boundary conditions $G = 0$ at the melting point and the enthalpy of fusion at the melting point.

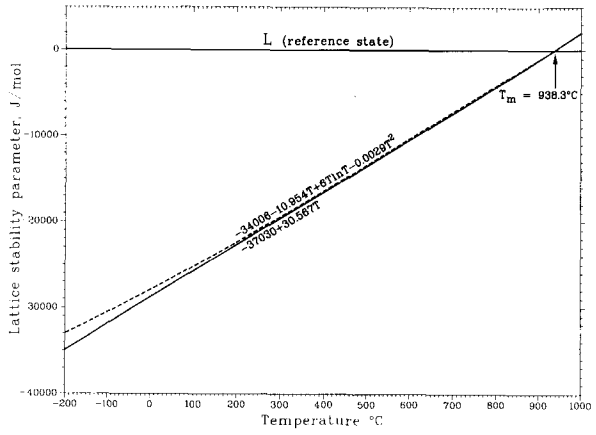

Fig. 5 Comparison of lattice stability parameters of Ge.

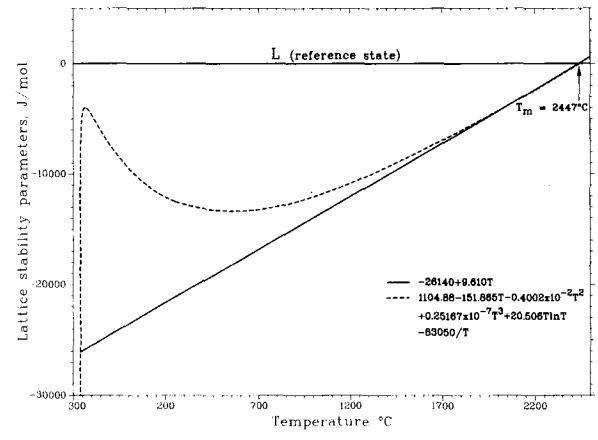

Fig. 6 Comparison of lattice stability parameters of Ir.

For a further comparison, the enthalpy of fusion of Ge was artificially taken to be 20 000 J/mol. The phase diagram calculated from

$$G^0(\text{Ge,diamond}) = -20\,000 + 16.509T \quad \text{J/mol}$$

and

$$\Delta_{mix}G^{ex}(\text{L}) = X(1-X)(-13\,354 + 14\,492X) \quad \text{J/mol}$$

is again almost identical to that calculated in [84Oka3]. As shown above, the liquidus boundary of (Ge) can be reproduced satisfactorily in spite of the substantial differences in the lattice stability parameters.

Sometimes, an assumption of non-zero C_p may result in an anomalous situation particularly if the applicable limit is not specified. The lattice stability parameter of fcc Ir given by [86Kar] is

$$G^0(\text{Ir,fcc}) = 1104.88 - 151.865T - 0.4002 \times 10^{-2}T^2 + 0.25167 \times 10^{-7}T^3 + 20.506T\ln T - 83\,050/T \quad \text{J/mol}$$

Apparently, a ΔC_p value in the literature was used (presumably [77Bar]). The trend of this expression is shown in Fig. 6 together with a simple lattice stability parameter obtained by assuming $\Delta C_p = 0$, *i.e.*,

$$G^0(\text{Ir,fcc}) = -26\,140 + 9.610T \quad \text{J/mol}$$

The complex expression is almost identical to the simple expression at temperatures near the melting point of Ir. [86Kar] used the complex lattice stability parameter for calculating the (Ir) liquidus of the Ag-Ir phase diagram (Fig. 7) from the melting point to the boiling point of Ag. The excess Gibbs energy of mixing of the liquid phase was obtained empirically. The calculated diagram using the simple lattice stability parameter is not materially different from that using the complex expression.

The above two examples and a review of the quite numerous thermodynamic models reported in the Alloy Phase Diagram Program for the binary system suggest that the $\Delta C_p = 0$ assumption is generally acceptable for calculating equilibrium phase diagrams. Major exceptions from this assumption may occur when magnetic interactions must be considered, or when metastable phase equilibria involving supercooled liquids are of interest.

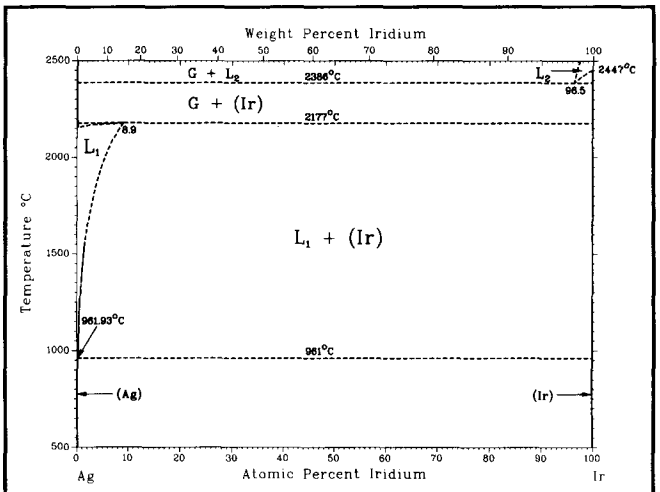

Fig. 7 Calculated Ag-Ir phase diagram [86Kar].

Because the lattice stability parameter of a given element must be universally applicable for calculation of phase equilibria in any binary (or higher-order) system involving that element, it is important that these parameters should be determined precisely in the future for as many elements as possible, including the allotropic crystal forms.

4.2 Selection of a Reference State

In the previous subsection, the liquid phase was assumed as the reference state of lattice stability parameters. Although the selection of a reference state is arbitrary, the expressions for lattice stability parameters may become more complex when an absolute reference state is used. For example, in calculating the Bi-Cu phase diagram, [90Tep] expressed the lattice stabilities of the

Table 1 Coefficients for Au-Te Liquid

i	0	1	2	3
a.....	296 920	-999 300	724 710	25 370
b.....	-4 574	15 298	-11 272	-70.08
c.....	676.597	-2 272.943	1 683.105	...
d.....	-0.392	1.324	-0.981	...

Note: $a = \Sigma_{i=0}^{4} a_i X^i$; $b = \Sigma_{i=0}^{4} b_i X^i$; $c = \Sigma_{i=0}^{2} c_i X^i$; $d = \Sigma_{i=0}^{2} d_i X^i$; and X = atomic fraction of Te.

Table 2 Au-Te Thermodynamic Properties

$G^0(\text{Au,L}) = 0$
$G^0(\text{Te,L}) = 0$
$G^0(\text{Au,fcc}) = -12\,550 + 9.3826T$
$G^0(\text{Te,L}) = -17\,490 + 24.200T$
$G^0(\text{AuTe}_2) = -24\,330 + 23.500T$

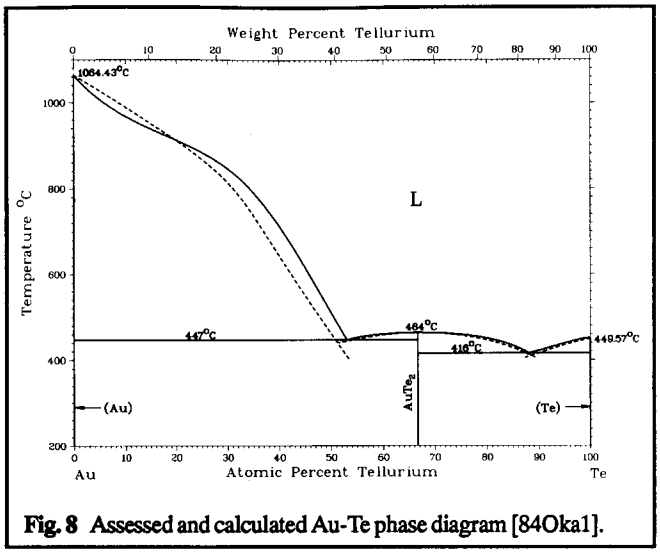

Fig. 8 Assessed and calculated Au-Te phase diagram [84Oka1].

liquid and the rhombohedral form of Bi in the temperature range between 298.15 and 544.52 K as follows:

$$G^0(\text{Bi,L}) = 3428.16 + 107.781519T - 28.4096529T\ln T + 1.2338888 \times 10^{-2}T^2 - 8.381598 \times 10^{-6}T^3 - 5.9726 \times 10^{-19}T^7 \quad \text{J/mol}$$

and

$$G^0(\text{Bi,rho}) = -7817.776 + 128.418885T - 28.4096529T\ln T + 1.2338888 \times 10^{-2}T^2 - 8.381598 \times 10^{-6}T^3 \quad \text{J/mol}$$

It is difficult to visualize the temperature dependence of these expressions. If, on the other hand, the liquid state is taken instead as the reference state, the lattice stability parameters become

$$G^0(\text{Bi,L}) = 0$$

and

$$G^0(\text{Bi,rho}) = -11\,245.936 + 20.637366T + 5.9726 \times 10^{-19}T^7 \quad \text{J/mol}$$

Thus, the expressions for the lattice stability parameters become more manageable when the liquid is selected as the reference state. The T^7 term still remains ($\Delta C_p = -2.5085 \times 10^{-17}T^6$), but its contribution is negligible. Following the discussion in Section 4.1, the above G^0(Bi,rho) function was compared against the $-11\,300 + 20.749T$ J/mol expression, which was derived from the enthalpy of fusion of Bi given in [83Cha]. The maximum energy difference between the two expressions in the temperature range where these expressions are applicable is only about 20 J/mol, and this is not discernible in a graph plotted against an ordinary scale (the maximum difference is only 0.3% of the full scale).

4.3 Omission of the Specific Heat of Mixing

When the specific heat of mixing is known and must be taken into account, the thermodynamic function expressions may become quite complex. If the temperature dependence of the specific heat of mixing of a liquid is known to the linear term as $X(1-X)(-c-2dT)$, the thermodynamic properties are given by

$$\Delta_{mix}G^{ex}(\text{L}) = X(1-X)(a + bT + cT\ln T + dT^2) \quad \text{Eq 4}$$

$$\Delta_{mix}H(\text{L}) = X(1-X)(a - cT - dT^2) \quad \text{Eq 5}$$

$$\Delta_{mix}S^{ex}(\text{L}) = X(1-X)(-b - c - c\ln T - 2dT) \quad \text{Eq 6}$$

$$\Delta_{mix}C_p(\text{L}) = X(1-X)(-c - 2dT) \quad \text{Eq 7}$$

according to the fundamental expressions given in section 2. Here, the odd coefficients ($-c$ and $-2d$) for the expression of $\Delta_{mix}C_p$(L) were chosen to make the final expression of $\Delta_{mix}G^{ex}$(L) as simple as possible. Because the integration in the derivation of $\Delta_{mix}H$(L) and $\Delta_{mix}S^{ex}$(L) is over T, coefficients a, b, c, and d could be of course composition dependent. As an example, the values for the Au-Te system are shown in Table 1. These rather complex expressions of the thermodynamic properties were derived by [77Ber] from the enthalpy and entropy of mixing data measured at several temperatures. Using these thermodynamic functions and the lattice stability parameters given in Table 2, [84Oka1] calculated the liquidus boundaries of the Au-Te phase diagram (dashed lines in Fig. 8). By substituting the coefficients for the composition dependence of a, b, c, and d, the Gibbs energy of mixing in an explicit form becomes

$$\Delta_{mix}G^{ex}(\text{L}) = X(1-X)(29\,6920 - 999\,300X + 724710X^2 + 25\,370X^3 - 10\,325X^4 + (-4574 + 15\,298X - 11\,272X^2 - 70.08X^3 + 8.060X^4)T + (676.597 - 2272.943X + 1683.105X^2)T\ln T + (-0.392 + 1.324X - 0.981X^2)T^2) \quad \text{J/mol} \quad \text{Eq 8}$$

As an alternative expression, a two-parameter subregular solution model was derived here from the liquidus phase boundary data.

$$\Delta_{mix}G^{ex}(\text{L}) = X(1-X)(-1960 - 42\,844X) \quad \text{J/mol} \quad \text{Eq 9}$$

The (Au) liquidus curve calculated using this two-parameter expression agrees perfectly well with the assessed boundary (solid line in Fig. 8). In terms of the number of parameters, this simple

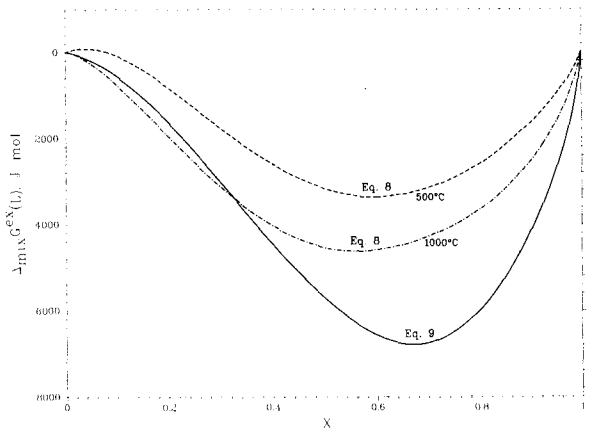

Fig. 9 Comparison of $\Delta_{mix}G^{ex}$(L) functions of Au-Te liquid.

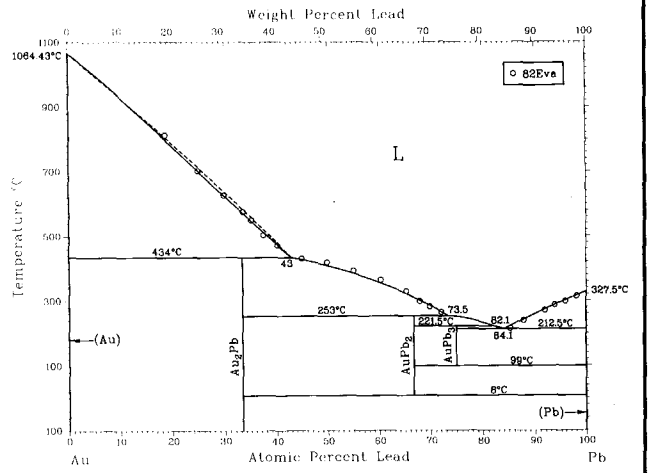

Fig. 10 Calculated Au-Pb phase diagram [84Oka2].

expression (Eq 9) is in sharp contrast to Eq 8 taking into account the specific heat of mixing. A glance at Eq 9 clearly suggests that the affinity between Au and Te becomes stronger at higher Te contents (probably to the extent that Au-Te associations have to be considered for $AuTe_2$ in the liquid state), whereas the former expression with sixteen coefficients provides no clue to the interaction chemistry. In Fig. 9 a comparison is made between the excess Gibbs energy of mixing expressed by Eq 8 and 9 at 500 and 1000 °C. The trends are similar, but the values given by the simple model (temperature independent) are generally more exothermic than those of the more complex model. However, this difference could be within the experimental uncertainty if one recalls the comments with respect to the Au-Cu and Au-Pb systems (as discussed in the previous section). At the least, however, the phase boundary calculated from the simple model agrees better with the experimental results in this case. When the simple model is adopted and the Au-rich eutectic point is chosen as an anchor point, the Gibbs energy of $AuTe_2$ becomes –43 577 + 44.624 J/mol*. The Te-rich eutectic point is calculated then to be 89 at.% and 382 °C.

Because it is difficult to decide which model is better in view of the limited thermodynamic data and the phase boundary data, the simple model, which does not take the specific heat of mixing into account, is clearly quite adequate for the present.

4.4 Omission of Excess Entropy of Mixing Term

Although the simpler model in the above example did not include the term for the excess entropy of mixing, the calculated diagram agrees well with the experimental results. In this subsection, the consequence of omitting the excess entropy of mixing term is considered using the Au-Pb system as an example.

[84Oka2] showed that the Au-Pb phase diagram can be reproduced quite satisfactorily by using the Gibbs energy of mixing for the liquid as summarized in the expressions given in Table 3. The corresponding calculated phase diagram is shown in Fig. 10.

Table 3 Au-Pb Thermodynamic Parameters

Excess Gibbs energy of mixing, J/mol

$\Delta_{mix}G^{ex}(L) = X(1-X)(-4174 - 14.078T)$

Lattice stability parameters and Gibbs energy of compound formation, J/mol

$G^0(Au) = -12\,550 + 9.383T$

$G^0(Pb) = -4799 + 7.990T$

$G(Au_2Pb) = -13\,527 + 9.053T$

$G(AuPb_2) = -8400 + 5.594T$

$G(AuPb_3) = -7246 + 5.511T$

As a further simplification, a regular solution model

$$\Delta_{mix}G^{ex}(L) = X(1-X)(-14\,115)\ \text{J/mol} \qquad \text{Eq 10}$$

was derived here by retaining the peritectic point of the (Au) liquidus at 43 at.% Pb and 434 °C. The difference in the L/[L + (Au)] liquidus boundary compositions calculated from these two models is within experimental uncertainty (Fig. 10). In the case of Au-Pb, the enthalpy of mixing of the liquid phase was known experimentally (although with substantial uncertainty as shown in Fig. 3). Therefore, the enthalpy term of $\Delta_{mix}G^{ex}$(L) could not be chosen arbitrarily. For example, the subregular solution model of Eq 10 requires a minimum value of -3529 J/mol for $\Delta_{mix}G^{ex}$(L) at 50 at.% Pb, which is too exothermic a value in comparison with all experimental data. The general difference is accounted for by the excess entropy of mixing term. However, this example suggests that if no experimental data were available for the enthalpy or the entropy of mixing in a given system, the excess entropy of mixing term might be ignored as far as the calculated phase diagram is concerned. In fact, the assumption of a zero excess entropy of mixing is often more realistic than the values obtained

* Mol in this article refers to mol of atoms, *i.e.*, g-atom.

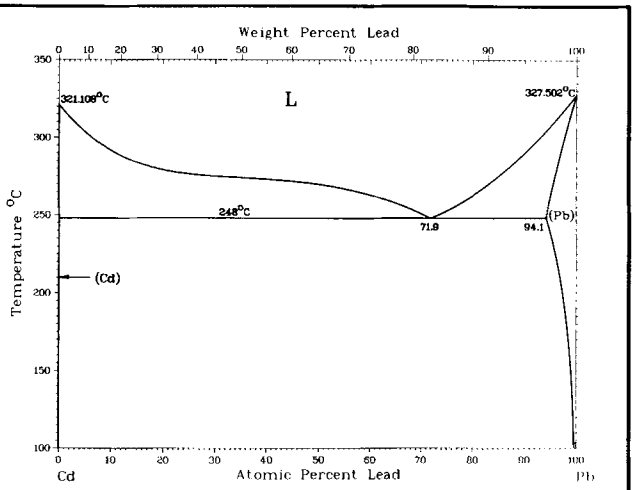

Fig. 11 Assessed Cd-Pb phase diagram [88Dut].

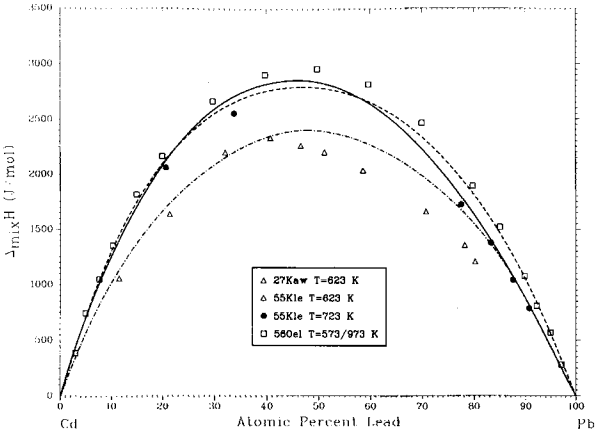

Fig. 12 Enthalpy of mixing of liquid Cd-Pb [88Dut].

by optimization of relatively inaccurate thermodynamic and phase diagram data, as discussed in sections 5 to 7.

When the excess entropy of mixing term is omitted, the excess Gibbs energy appears to consist of only the enthalpy term. However, the actual magnitude of the enthalpy of mixing may be substantially altered, because the excess Gibbs energy term now includes also the averaged $T\Delta_{mix}S^{ex}$ term over the temperature range being considered.

4.5 Omission of Higher-Order Terms

The Cd-Pb phase diagram was modeled by [88Dut] using a Gibbs energy of mixing function as follows:

$$\Delta_{mix}G^{ex}(L) = (15\,609 - 6.450T)X + (-38\,034 + 22.887T)X^2 + (60\,234 - 40.261T)X^3 + (-70\,925 + 37.607T)X^4 + (44\,124 - 15.193T)X^5 + (-11\,010 + 1.410T)X^6 \quad \text{J/mol}$$

The twelve coefficients in this expression were obtained by optimization of the available thermodynamic data. The calculated phase diagram (Fig. 11) using this expression was considered to agree very well with the experimental diagram. However, as already mentioned, the general trend of the Gibbs energy function is difficult to comprehend or analyze from this expression. By separating the enthalpy and entropy terms and rearranging each in the ascending order of the power of X, the following equation is obtained:

$$\Delta_{mix}G^{ex}(L) = X(1-X)(15\,609 - 22\,425X + 37\,809X^2 - 33\,116X^3 + 11\,010X^4 - (6.450 - 16.437X + 23.824X^2 - 13.783X^3 + 1.41X^4)T) \text{ J/mol} \quad \text{Eq 11}$$

Even with this rearrangement, the trend of this function is difficult to see. As an alternative, a rather simplified expression has been derived below, entirely omitting the excess entropy term, in conformity with the view expressed in the previous subsection:

$$\Delta_{mix}G^{ex}(L) = X(1-X)(12\,030 - 8310X + 6870X^2) \text{ J/mol} \quad \text{Eq 12}$$

Together with the lattice stability parameter of cadmium $G^0(Cd) = -6200 + 10.433T$ J/mol, the phase diagram in [88Dut] can be reproduced almost exactly using this three-parameter model. However, because the excess entropy of mixing term is not considered in the expression, the enthalpy term may involve a substantial uncertainty. Figure 12 shows the enthalpy of mixing of the present formulation compared with the experimental data and the expressions quoted in [88Dut]. Clearly, the present expression is within the scatter of the experimental scatter. If the expression of [88Dut] for $\Delta_{mix}H$ (dashed line in Fig. 12) is accurate, the difference between this line and the present expression (dash-dot line) can be explained in terms of the excess entropy of mixing. So, at least for the purpose of phase diagram modeling, simple expressions may be more informative than the more complex ones.

Durning the search for a simple model for the above system, an attempt was made to find a Gibbs energy function having only two parameters (rather than three) that would still adequately reproduce the (Cd) liquidus. However, two-parameter models always developed a miscibility gap in the liquid phase.

5. Examination of Thermodynamic Parameters

5.1 Unnecessary Accuracy

As illustrated in section 3, the thermodynamic data in the literature are likely to be often unreliable. It follows that the corresponding thermodynamic parameters need not be given to too many effective digits. For example, [84Nay] calculated the Mg-Sn phase diagram using

$$\Delta_{fus}G(Mg_2Sn) = 7955.21307607 + 86.614844T - 13.560819T\ln T \quad \text{J/mol}$$

By equating $\Delta_{fus}G(Mg_2Sn) = 0$, this expression leads to a melting point of 769.67000 °C. If the effective digits are limited to four, the melting point becomes 769.7 °C. The omission of the trailing numbers causes only insignificant changes in the value of the Gibbs energy function, or the calculated phase diagrams.

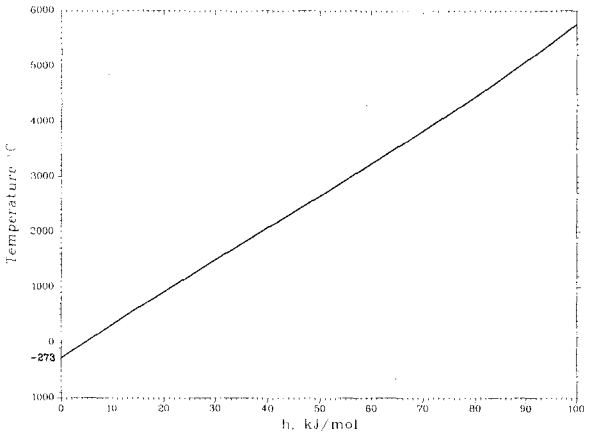

Fig. 13 Critical point temperature of a miscibility gap of a regular solution. This figure illustrates the relationship between the critical temperature of a miscibility gap (of both solid and liquid phases) and the value of h of a regular solution.

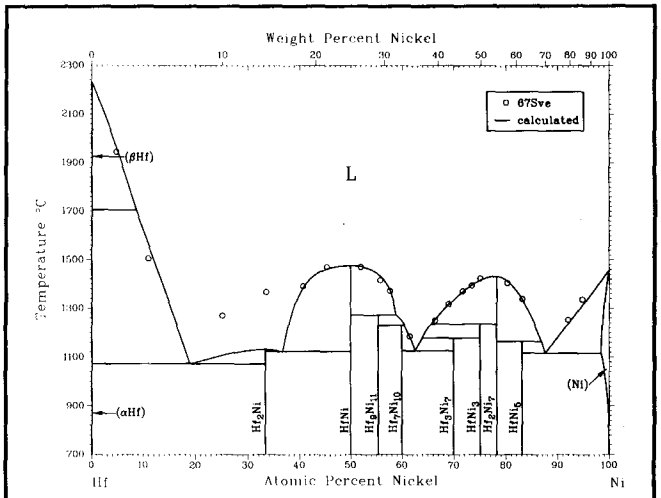

Fig. 14 Calculated Ni-Hf phase diagram [90Zen].

Table 4 Erroneous Au-Pb Thermodynamic Parameters

$\Delta_{mix}H(L) = -6\,200 - 15\,144X + 19.287XT$ J/mol
$\Delta_{mix}S^{ex}(L) = 9.8486 - 12.127X$ J/mol
$\Delta_{mix}G^{ex}(L) = -6\,200 - 15\,144X - (9.8486 - 31.160X)T$ J/mol

5.2 Magnitude of Parameters

Sometimes, the general validity of a thermodynamic model can be examined simply by looking at the magnitudes of the coefficients of the polynomial expressions used in the model. A good thermodynamic parameter is unlikely to have extremely large or extremely small values. In addition, there has to be some relevance relative to other parameters used in the given system, as illustrated below.

When a phase diagram is calculated with a thermodynamic model, the parameters in the model are quite often derived from the experimentally established boundaries of the phase diagram. If some of the boundaries are unrealistic, the corresponding thermodynamic parameters will also be unrealistic. However, because the phase diagram calculated using these unrealistic parameters can be quite similar to the experimental diagram, the fact that the thermodynamic model involves unusual parameters may attract little attention. Although it is impossible to set clear cut limits for the maximum permissible values of, say, the enthalpy of mixing of a binary liquid, a general idea can be obtained from the semi-empirical estimates given by [80Mie]. As an exceptionally large value (in absolute magnitude), [80Mie] predicted –377 kJ/mol for the enthalpy of solution of Y in liquid Pd (partial enthalpy of mixing of Y in liquid Pd). Indeed, there are not many situations where the value can be lower than –300 kJ/mol (see also [83Nie]). On the positive side, the enthalpy of mixing, in terms of h(L), cannot usually exceed much over +20 kJ/mol (for Au-based systems) without developing a miscibility gap [91Oka]. Therefore, if the partial molar quantity a (at $X = 0$) or $a + b + c \ldots$ (at $X = 1$) of the enthalpy of mixing of the liquid in terms of h(L) = $(a + bX + cX^2 + \ldots)$ is considerably outside the range of –300 to + 20* kJ/mol, the model is likely to be unrealistic. In this light, an example of a model with unusual parameters is shown in section 6.

When a binary system involves several compounds, a comparison of the enthalpy terms of the compounds provides another method of examining the consistency of the thermodynamic model. If one of the values is substantially smaller (large negative value) than the others, the compound is clearly very stable and other compounds may become unstable at low temperatures. This situation is also illustrated with an example in section 6.

5.3 Temperature Dependence of Enthalpy and Excess Entropy of Mixing

As emphasized in subsection 4.3, the temperature dependencies of the enthalpy of mixing and the excess entropy of mixing are not independent. For example, if h is assumed to be linearly dependent on temperature ($c \neq 0$), s must have the $T\ln T$-type form temperature dependence. If s is linearly dependent on temperature ($d \neq 0$), h must have the T_2-type form.

Table 4 shows one of the thermodynamic models for the Au-Pb system as used in [84Oka2] to represent experimental thermodynamic data.

Although the $\Delta_{mix}H$(L) function represents the experimental enthalpy of mixing data quite well and the $\Delta_{mix}G^{ex}$(L) function has parameters with typical values, the relationship between $\Delta_{mix}H$(L) and $\Delta_{mix}S^{ex}$(L) is not satisfactory.

* This limit applies only to systems that do not mix in the liquid state. The value may be higher for bonary systems with high liquidus temperatures. Figure 13 illustrates the relationship between the critical temperature of a miscibility gap (of both solid and liquid phases) and the value of h of a regular solution.

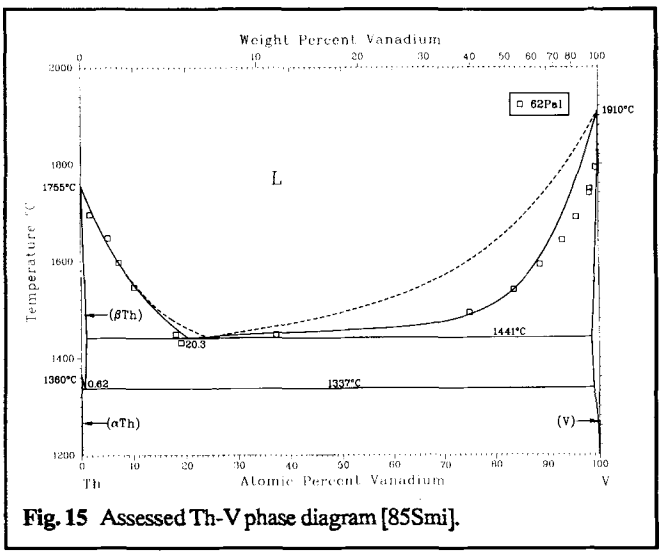

Fig. 15 Assessed Th-V phase diagram [85Smi].

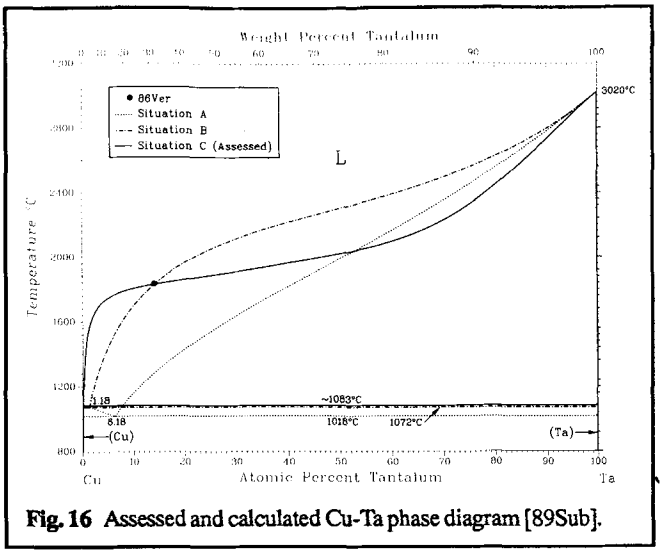

Fig. 16 Assessed and calculated Cu-Ta phase diagram [89Sub].

Table 5 Th-V Thermodynamic Parameters

Excess Gibbs energy of mixing, J/mol

$\Delta_{mix}G^{ex}(L) = X(1-X)(28\,550 - 3725X)$

Lattice stability parameter, J/mol

$G^0(Th) = -13\,800 + 6.8T$

$G^0(V) = -21\,500 + 9.85T$

If the excess Gibbs energy of mixing is expressed in the form $\Delta_{mix}g^{ex}(L) = A(X) - B(X)T$, then $h(X,T) = A(X)$ and $s(X,T) = B(X)$. In other words, h and s are temperature independent. If all or a part of $B(X)T$ represents the temperature dependence of h, the coefficient c in Eq 5 is not zero. Thus, Eq 4 requires that $\Delta_{mix}g^{ex}(L)$ involves a $cT\ln T$ term, which is contradictory to the initial assumption. Therefore, only the expression of $\Delta_{mix}g^{ex}(L)$ is valid in Table 4.

6. Examples of Unlikely Thermodynamic Models

This section discusses, examples of thermodynamic models that involve parameters with unusual magnitudes.

6.1 Unusual Gibbs Energy of Formation of a Compound

[90Zen] calculated the Ni-Hf phase diagram (Fig. 14) using optimized thermodynamic parameters derived from the experimental data of [67Sve] and lattice stability parameters of [75Kau]. [90Zen] obtained the Gibbs energies of formation as follows:

for $NiHf_2$,

$G(NiHf_2) = -111\,245.8 + 61.665T$ J/mol

and for NiHf,

$G(NiHf) = -289.5 - 15.317T$ J/mol

Given the large first term, the Gibbs energy of $NiHf_2$ becomes too low at low temperatures (consider $T = 0$), and accordingly, NiHf (actually also all the other compounds as well) become unstable according to this model. [90Zen] also obtained rather unrealistic temperature and composition dependencies in the interaction parameters of the liquid and (Ni) phases:

$$\Delta_{mix}G^{ex}(L) = X(1-X)(-189\,147.8 + 435\,064X - 392\,611.8X^2) \quad \text{J/mol}$$

$$\Delta_{mix}G^{ex}(Ni) = X(1-X)(-1\,898\,846.7 + 15\,808\,247.8X - 17\,902\,408.8X^2 + 2249.468T) \quad \text{J/mol}$$

As can be seen immediately, the value of the partial enthalpy of mixing at 0 at.% Ni for the (Ni) phase (–1 898 846.7 J/mol) is unacceptable. In the model, this extremely large negative enthalpy of mixing is compensated for by the extremely large negative excess entropy of mixing (positive contribution to the Gibbs energy). For example, at 50 at.% Ni and 1500 K, contribution to the Gibbs energy from the enthalpy and the excess entropy terms are –382 418.8 and 843 550 J/mol, respectively.

6.2 Unusual Excess Entropy of Mixing

The excess entropy of mixing of a liquid phase cannot have a very large positive value. If this is the case, the contribution of the excess entropy of mixing in lowering the excess Gibbs energy becomes too large at high temperatures. If the gas phase is an ideal mixture (reasonable assumption), the Gibbs energy of the gas phase decreases only at a rate ~100 J/mol · K (rough average of entropy of vaporization for metallic elements) with respect to the liquid phase. Therefore, if $\Delta_{mix}S^{ex}(L)X(1-X)$ is greater than ~100 J/mol · K at any X, the liquid state becomes more stable than the gas phase at high temperatures, which is unlikely. Therefore, any model having $s(L)$ greater than ~400 J/mol is impossible. Thermodynamic models of metallic systems with $s(L)$ greater than 5 J/mol are rare. Similarly, a $s(L)$ value less than –10 J/mol is also rare. Thermodynamic models with $s(L) = 0$ are most common.

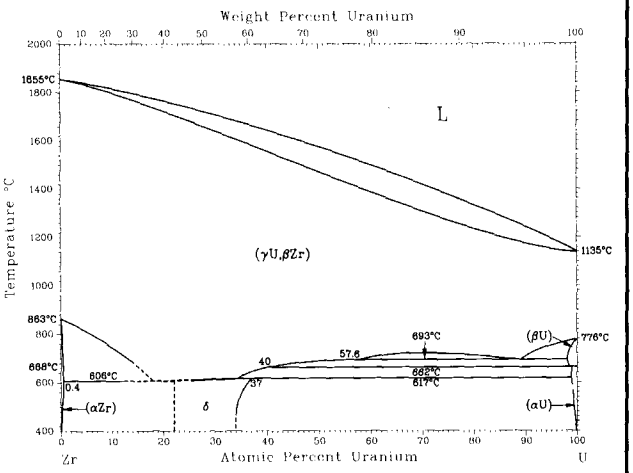

Fig. 17 Assessed U-Zr phase diagram [89She].

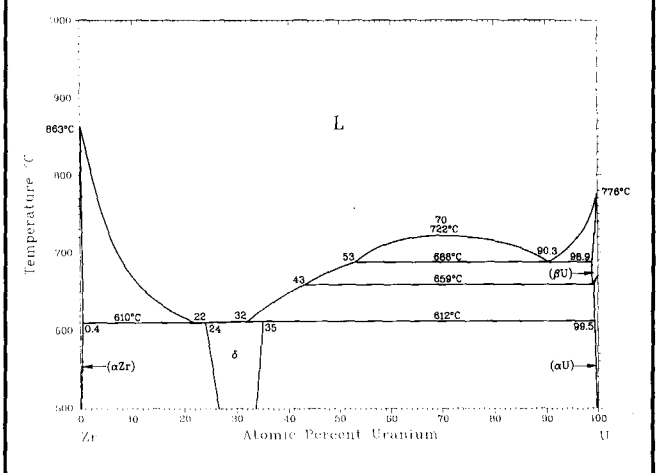

Fig. 18 Calculated Zr-U phase diagram [91Oga].

Table 6 Cu-Ta Thermodynamic Data

Lattice stability parameter, J/mol

G^0(Cu,fcc) = –13 054 + 9.613T
G^0(Ta,bcc) = –36 570 + 11.105T

Excess Gibbs energy of mixing, J/mol

Situation A: $\Delta_{mix}G^{ex}(L) = X(1-X)(9000-2000X)$
Situation B: $\Delta_{mix}G^{ex}(L) = X(1-X)(28\,771)$
Situation C: $\Delta_{mix}G^{ex}(L) = X(1-X)(246\,419-103.34T)$

From [89Sub].

Table 7 Thermodynamic Properties of Zr-U

Lattice stability parameters, J/mol

G^0(Zr,L) = 0
G^0(U,L) = 0
G^0(Zr,bcc) = –20 930 + 9.84T
G^0(U,bcc) = –8 520 + 6.07T

Gibbs energy of mixing, J/mol

$\Delta_{mix}G^{ex}(L) = X(1-X)(126\,250-24\,100X-71.44T)$
$\Delta_{mix}G^{ex}(bcc) = X(1-X)[95\,879-218\,398X+236\,840X^2 - (87.93-228.18X+235.88X^2)T]$

From [91Oga].

Figure 15 shows the Th-V phase diagram calculated by [85Smi], which was based on the experimental data obtained by [62Pal]. [85Smi] assumed, in calculating the Th-V phase diagram, that the excess Gibbs energy of mixing in the liquid is:

$$\Delta_{mix}G^{ex}(L) = X(1-X)[426\,243 + 531\,490X - (233.316 + 307.260X)T] \quad \text{J/mol}$$

This very large positive excess entropy of mixing (s = 233.316 + 307.260X J/mol · K) may have been unnoticed, because it is compensated for by an equally large enthalpy term (partial enthalpy of mixing at X = 1 is 957 733 J/mol, which is 34 times as large as the prediction of [83Nie]) assumed to be valid at temperatures where the phase diagram was calculated.

A much simpler, yet equally effective thermodynamic function may be derived by assuming that the liquidus data reported by [62Pal] are systematically too low by ~100 °C, which is quite plausible considering the large deviation in the [62Pal] data of the melting point of pure V from the currently accepted value (see Fig. 15). Given this assumption, a subregular solution model summarized in Table 5 reproduces the data of [62Pal] quite well (with 100 °C offset), as shown in Fig. 15. The pure component lattice stability parameters were taken from [85Smi].

6.3 Unusual Enthalpy of Mixing

To determine the entire liquidus of the Cu-Ta system (Fig. 16), [89Sub] compared three thermodynamic models (Table 6) and selected the situation C, where the enthalpy of mixing is >246 kJ/mol (in terms of h(L)). However, as pointed out in subsection 5.2, h(L) of a liquid phase having continuous solubility cannot exceed a value much above 20 kJ. Consistent with this, the prediction of [83Nie] for h(L) is 7 to 9 kJ/mol (situation A). Thus, the value used in situation C is possibly some 30 times as large as the likely actual value. Of course, to compensate for the very high h(L) value, the situation C model includes an unusually large negative contribution from the excess entropy term (see previous section). [89Sub] decided that the situation C model is more realistic than the other two situations by comparing the calculated liquidus with experimental data. However, other possibilities were not considered, *e.g.*, that the experimental phase boundary data may be in error, or that the solubility of Cu in (Ta) is in fact not negligible.

6.4 Unusual Sign in the Enthalpy of Mixing

Fig. 17 shows the Zr-U phase diagram assessed by [89She], while Fig. 18 shows a phase diagram calculated by [91Oga] using the

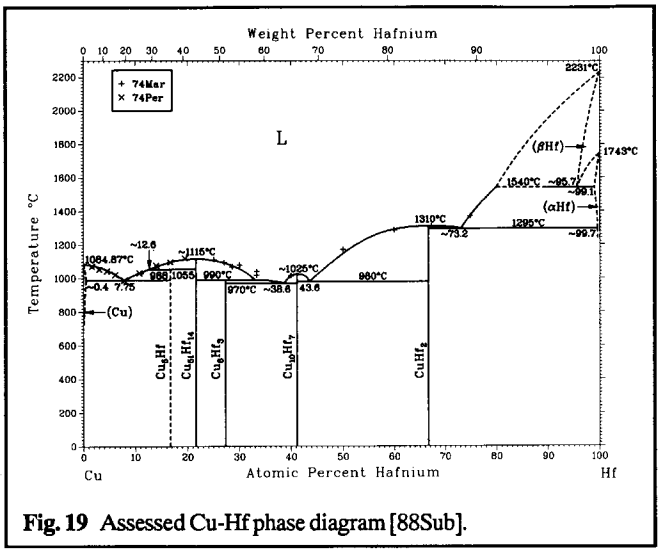

Fig. 19 Assessed Cu-Hf phase diagram [88Sub].

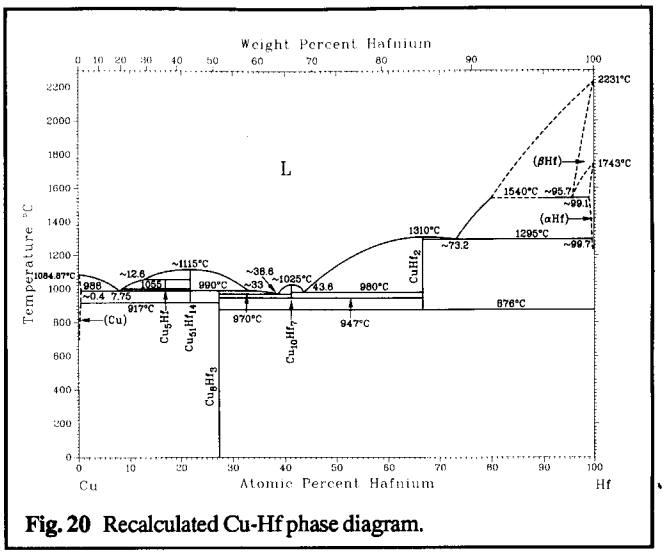

Fig. 20 Recalculated Cu-Hf phase diagram.

Table 8 Cu-Hf Thermodynamic Properties

Lattice stability parameters for Cu, J/mol

$G^0(Cu,L) = 0$

$G^0(Cu,fcc) = -13\ 054 + 9.613T$

Lattice stability parameters for Hf, J/mol

$G^0(Hf,L) = 0$

$G^0(Hf,bcc) = -23\ 390 + 9.341T$

$G^0(Hf,cph) = -29\ 300 + 12.272T$

Integral molar Gibbs energies, J/mol

$G^0(L) = X(1-X)[-77\ 800 - T(83.009 + 248.426X - 596.531X^2 + 328.495X^3)]$

$\Delta_f G(Cu_5Hf) = -33\ 512 - 2.137T$

$\Delta_f G(Cu_{51}Hf_{14}) = -69\ 089 + 11.983T$

$\Delta_f G(Cu_8Hf_3) = -210\ 207 + 126.04T$

$\Delta_f G(Cu_{10}Hf_7) = -23\ 890 - 27.682T$

$\Delta_f G(CuHf_2) = -80\ 005 + 16.393T$

From [88Sub].

diagram of [89She] as input data. The most obvious difference in these two phase diagrams is in the initial slopes of (βZr,γU)/[(βZr,γU) + (αZr)] and (βZr,γU)/[(βZr,γU) + (βU)]. Considering that the solid solubility of U in (αZr) is small (Fig. 17) and that the enthalpy of βZr/αZr transformation is small (~4 kJ/mol) [83Cha], the initial slope is expected to be steep [91Oka], in agreement with [91Oga]. The same situation is observed on the U side of the phase diagram. Therefore, the diagram of [91Oga] appears to be preferable to that of [89She]. However, the thermodynamic model used by [91Oga] (Table 7) includes unusual sets of parameters.

The positive and large enthalpy of mixing of the liquid phase ($g^{ex}(L) = 126\ 250 - 24\ 100X$ J/mol) is unusual for a system such as Zr-U with a smooth and continuous liquidus, which is often indicative of exothermic mixing of two elements (*i.e.*, negative enthalpy of mixing). As a matter of fact, [83Nie] estimated for this system the enthalpy of mixing to be $-13\ 000X(1-X)$ J/mol. The large positive enthalpy term is canceled by an even larger enthalpy term (in the temperature range where the liquidus is involved) in the Gibbs energy function of [91Oga]. To allow a normal set of the liquidus and solidus existing at high temperatures and to allow for the formation of a miscibility gap at low temperatures, the Gibbs energy of mixing for the bcc (βZr,γU) also is made to have an unusual temperature dependence, as given in Table 7. The difficulty in obtaining a reasonable set of thermodynamic functions may indicate that the phase diagram used as the input data has to be reinvestigated.

7. Examples of Unlikely Phase Diagrams Calculated by Thermodynamic Models

Recently, [91Oka] discussed in some detail many phase diagrams that are thermodynamically improbable. As a sequel to this work, it can be stated that if a calculated phase diagram does not meet some criteria elaborated by [91Oka], this is a strong indication that something may be wrong with the thermodynamic model, or the calculation process. A few examples are considered below.

7.1 Mixed Degrees of Curvature in the Liquidus

[91Oka] showed that the general curvature of the liquidus of a compound near its melting point cannot be much different from that of the neighboring compounds in the phase diagram. A compound with a sharper liquidus will be associated with a coefficient in the enthalpy part of the Gibbs energy equation that will make it unstable at a lower temperature (*i.e.*, decompose eutectoidally). Figure 19 shows the Cu-Hf phase diagram calculated by [88Sub]. Apparently, the liquidus of $Cu_{10}Hf_7$ falls off more steeply than that of the neighboring Cu_8Hf_3. Therefore, the thermodynamic model employed by [88Sub] (Table 8) is open to some question. Inspection of Table 8 immediately confirms that Cu_8Hf_3 is predicted to be extremely stable at low temperatures (*i.e.*, at T = 0 K, the Gibbs energy of formation of Cu_8Hf_3 is –210 207

Table 9 Metastable Melting Point of Low-Temperature Allotrope

Element	Normal melting point, °C	Melting point of low-temperature phase, °C	Difference, °C
Am	1176	1146	30
Be	1289	1286	3
Ca	842	788	54
Ce	798	771	27
Cm	1345	1332	13
Co	1495	1424	71
Dy	1412	1403	9
Fe	1538	1529	9
Gd	1313	1290	23
Hf	2231	2133	98
La	918	900	18
Mn	1246	1230	16
Nd	1021	970	51
Np	639	606	33
Pa	1572	1408	164
Pr	931	885	46
Pu	640	571	69
Sc	1541	1491	50
Sm	1074	1030	44
Sr	769	741	28
Tb	1356	1334	22
Th	1755	1658	97
Ti	1670	1408	262
Tl	304	297	7
U	1135	987	148
Y	1522	1508	14
Yb	819	814	5
Zr	1855	1593	262

J/mol). Because this value dominates the system, all the other compounds are unlikely to remain as stable compounds at low temperatures. In addition, the Gibbs energy of mixing of the liquid is also unusual in the [88Sub] model: the enthalpy term is typical of a regular solution expression, whereas the entropy term is strongly composition dependent. These problems aside, the Cu-Hf phase diagram was recalculated using the values given in Table 8. The result is shown in Fig. 20. As expected, the liquidus boundaries are almost the same as shown by [88Sub], but also as expected from the sharpness of the liquidus and from the Gibbs energy functions, all compounds except Cu_8Hf_3 became unstable at low temperatures. There are no reports in the literature that this is in fact the correct picture, so the thermodynamic modeling needs an appropriate modification.

7.2 Problem of the Initial Slope

The question of the initial slope of the liquidus near both sides of the pure components in a binary system was discussed in detail by [91Oka]. In one of the examples, it was pointed out that the proposed initial slopes of (Al) and (Ca) in the Al-Ca phase diagram (Fig. 21), as calculated by [88Itk], appear to be unrealistic by the simple test that the initial liquidus slope of a metallic terminal phase having little or no solid solubility should cut the vertical temperature axis on the other side of the phase diagram approximately between 0 and 273 K (*i.e.*, 0 °C). A closer examination of the thermodynamic model used by [88Itk] shows

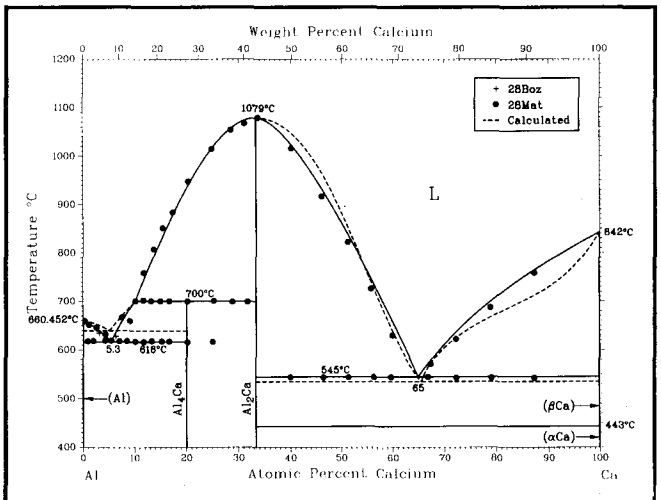

Fig. 21 Assessed and calculated Al-Ca phase diagram [88Itk].

that the excess Gibbs energy of mixing of the liquid Al-Ca was expressed by

$$\Delta_{mix}G^{ex}(L) = X(1-X)[-103\,877 - 156\,696X + 545\,132X^2 - 352\,560X^3 - T(-65.38 - 4.32X + 194.6X^2 - 168.32X^3)] \quad \text{J/mol}$$

where the enthalpy term was derived from experimental data and the entropy term was based on optimization of the phase diagram. A recalculation of the Al-Ca phase diagram attempted here using the thermodynamic parameters given by [88Itk] supports the calculated phase diagram very well except in the ranges very near to the pure elements, where the calculated slopes are not in conformity with the "slope rule" of [91Oka]. Hence, the appearance of a deviation in Fig. 21 from the required initial slope is probably due to a drawing problem, or perhaps the phase boundaries were simply not calculated near the pure elements. The significant deviation of the liquidus from the required initial slope is clearly caused by the assumed large entropy term. However, since the entropy term was derived itself from an assumed phase diagram, the assessment becomes circuitous. On the other hand, if a substantial homogeneity range is given to the (βCa) phase (although it must be confirmed), the difficulties mentioned here can be alleviated. So, even if there was no computational error in [88Itk], the apparently anomalous deviation of the initial slope from the clearly established trend in [91Oka] reveals possible problems for the entire model.

7.3 Problem of Metastable Melting Point of a Pure Element

When an element exists in two allotropic forms, consistency regarding the metastable melting point of the low-temperature forms must be considered. If ΔC_p between the two allotropic forms is assumed to be zero, the metastable melting point of the low-temperature phase is given by

$$T = \frac{\Delta H_m + \Delta H_t}{\frac{\Delta H_m}{T_m} + \frac{\Delta H_t}{T_t}}$$

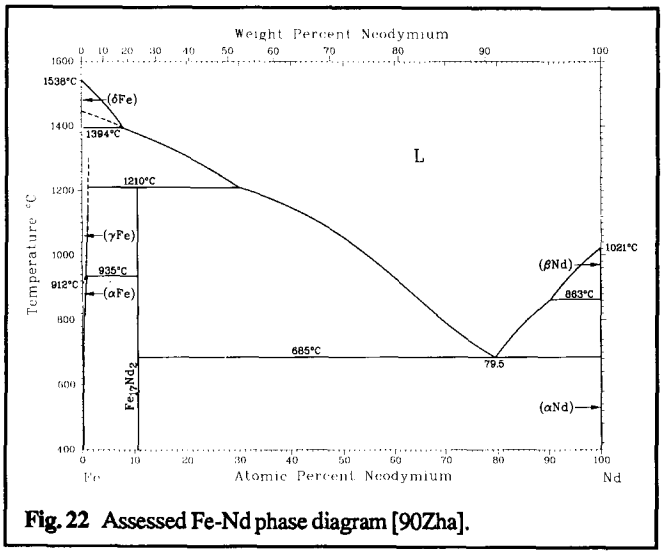

Fig. 22 Assessed Fe-Nd phase diagram [90Zha].

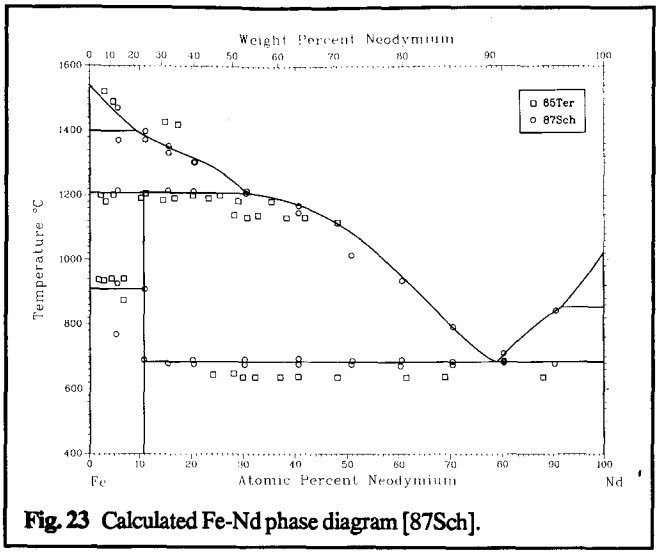

Fig. 23 Calculated Fe-Nd phase diagram [87Sch].

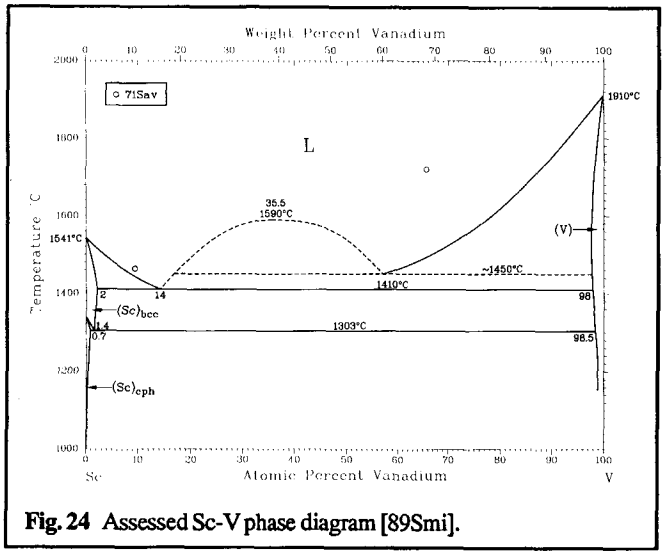

Fig. 24 Assessed Sc-V phase diagram [89Smi].

where T_m is the melting point of the high-temperature phase, T_t is the allotropic transformation temperature, ΔH_m is the enthalpy of fusion of the high-temperature phase, and ΔH_t is the enthalpy of transformation. Table 9 shows the melting point of the low temperature phases of elements with more than two allotropic forms calculated by substituting in the equation above the melting points and the transformation temperatures [90Mas] and the values of the enthalpies of fusion and transformation [83Cha], respectively.

The calculated metastable melting point may be slightly different if a different ΔC_p value is used. However, the difference in the melting point is usually very small as already shown in Section 4.1. When an element exists in more than two allotropic forms, the metastable melting point of the still lower temperature phases can be calculated similarly. However, the assumption of $\Delta C_p = 0$ may not always be reasonably appropriate (*e.g.*, due to the influence of the magnetic interaction in Fe) and such a low-temperature phase usually does not have an associated liquidus anyway. Therefore, only the metastable melting points of the first low-temperature phases are given in Table 9.

According to this table, the difference between the melting point of the high temperature phase and the low-temperature phase of an element is surprisingly small, although there are exceptions (Ti, Zr, Pa, U, etc.). For example, the melting point of γFe is only 9 °C below the melting point of δFe. Therefore, the melting point of δFe in the assessed Fe-Nd phase diagram by [90Zha] (Fig. 22) appears to be too low. This phase diagram was adopted from a thermodynamically calculated phase diagram of [87Sch] (Fig. 23), in which the liquidus of (γFe) appears to be extrapolated smoothly to the metastable melting point of γFe(1529 °C). Hence, it appeared at first that there was a problem in redrawing. However, it turned out that the problem was not so simple, as described below.

The lattice stability parameters of Fe phases given by [87Sch] were:

$$G^0(\mathrm{L}) = -10\,839.7 + 245.302T$$

$$G^0(\delta\mathrm{Fe}) = 1224.8 + 100.620T + 23.514T(1 - \ln T) - 8.795 \times 10^{-3}T^2/2 + 1.5472 \times 10^{-3}/2T + 0.3536 \times 10^{-6}T^3/6$$

$$G^0(\gamma\mathrm{Fe}) = -237.6 + 107.752T + 24.664T(1 - \ln T) - 7.715 \times 10^{-3}T^2/2 + 1.5472 \times 10^{-3}/2T + 0.3536 \times 10^{-6}T^3/6$$

Unfortunately, these expressions are erroneous, because they do not yield the melting points of δFe and γFe at all and they place the δFe to γFe transformation temperature at 2070 °C (instead of 1394 °C). In addition, the excess Gibbs energy of mixing of the liquid phase used by [87Sch] was:

$$G^{ex}(\mathrm{L}) = X(1-X)[246\,708.8 - 705\,805.6X + 589\,650.4X^2 - T(178.334 - 359.514X + 341.888X^2)] \quad \mathrm{J/mol}$$

Table 10 Be-Co Thermodynamic Parameters

Excess Gibbs energy of mixing, J/mol

$\Delta_{mix}G^{ex}(L) = -X_{Co}X_{Be}(-16\,736X_{Co} + 25\,104X_{Be})$

$\Delta_{mix}G^{ex}(bcc) = -X_{Co}X_{Be}(-16\,736X_{Co} - 23\,012X_{Be})$

Lattice stability parameter, J/mol

$G^0(Co,bcc) = -13\,894 + 9.16296T$

$G^0(Be,bcc) = -10\,418 + 6.694T$

From [84Kau].

Table 11 Possible Be-Co Thermodynamic Parameters Used

Excess Gibbs energy of mixing, J/mol

$\Delta_{mix}G^{ex}(L) = -X_{Co}X_{Be}(16\,736X_{Co} + 25\,104X_{Be})$

$= X(1-X)(-16\,736 - 8363X)$

$\Delta_{mix}G^{ex}(bcc) = -X_{Co}X_{Be}(16\,736X_{Co} + 23\,012X_{Be})$

$= X(1-X)(-16\,736 - 6726X)$

Table 12 Co-Be Thermodynamic Parameters

Excess Gibbs energy of mixing, J/mol

$\Delta_{mix}G^{ex}(L) = X(1-X)(-28\,181 - 27\,105X)$

$\Delta_{mix}G^{ex}(bcc) = X(1-X)(-18\,998 - 38\,238X)$

Lattice stability parameter, J/mol

$G^0(Co,bcc) = -12\,877 + 7.606T$

$G^0(Be,bcc) = -12\,600 + 8.067T$

From [87Oka3].

Apparently, both the enthalpy and the entropy terms are too large according to the discussions in subsections 6.2 and 6.3. Thus, the thermodynamic model of [87Sch] includes unresolved problems. Because the initial slope of (δFe) in the diagram of [87Sch] does not follow the general trend for Fe-rare earth systems [92Oka], the most obvious conclusion is that the assumption of no solubility of Nd in (δFe) made by [87Sch] is the main reason for the difficulty in the thermodynamic modeling.

7.4 Problem of a Liquidus Showing a Trend That Will Cross the Pure Element Line

The liquidus of (V) in the Sc-V phase diagram calculated by [89Smi] (Fig. 24) is almost horizontal near the eutectic at 14 at.% V. When extrapolated to the Sc-rich side, the liquidus appears to cross the 0 at.% V line, unless an abrupt change of slope is introduced in the metastable range. As pointed out in [91Oka], because both the crossing of the 0 at.% V line and the abrupt change of slope are thermodynamically unacceptable, the thermodynamic model developed for the Sc-V system may require modification.

The excess Gibbs energy of mixing of the liquid Sc-V derived by [89Smi] is of the form

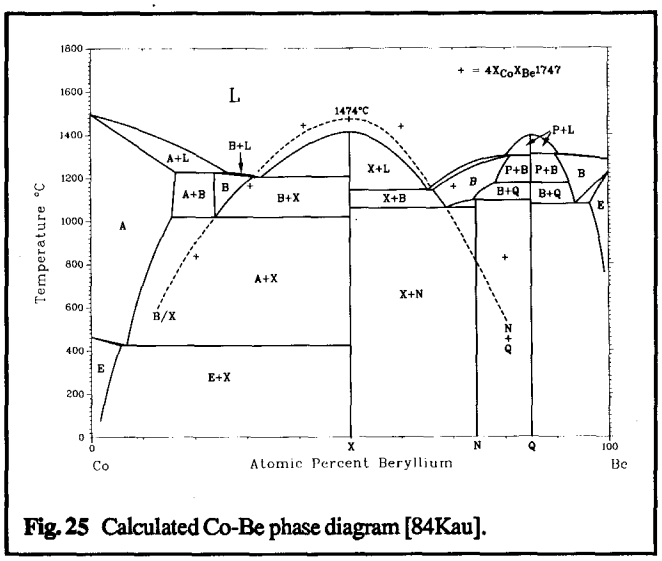

Fig. 25 Calculated Co-Be phase diagram [84Kau].

$\Delta_{mix}G^{ex}(L) = X(1 - X)(34\,754 - 14\,342X)$ J/mol

Since the positive interaction parameter (h) is proposed to be greater than 20 kJ/mol in the entire composition range (see subsection 5.2), the existence of a miscibility gap may be expected. Actually, according to this model, a critical point occurs at 35.5 at.% V and 1590 °C. The calculated diagram should then appear as shown with dotted lines in Fig. 24 (as corrected in [90Mas]). Most likely, the liquidus in [89Smi] was not calculated in the narrow temperature range between the monotectic temperature and the eutectic temperature, thereby missing the miscibility gap. However, the experimental data of [71Sav], on which the thermodynamic model of [89Smi] is based, seems to indicate a simple eutectic system without a miscibility gap. Taking into account the fact that the calculated liquidus does not agree well with the data points of [71Sav] (Fig. 24), the thermodynamic model requires further revisions. Alternatively, the experimental data in the critical regions of the phase diagram should be rechecked.

7.5 Problem of Phase Continuation

The Co-Be phase diagram (Fig. 25) provides an interesting situation in which the same bcc phase occurs in three different portions at high temperatures. Accordingly, the continuation of this phase in the metastable ranges, when separated by intermediate phases, is expected and becomes of interest. In Fig. 25 [84Kau], possible problems are evident in the phase diagram even without modeling calculation. The three small single-phase regions marked B are all clearly part of a single bcc phase field separated by phases X and Q. If there were no X and Q, liquidus and solidus boundaries of the bcc B phase would be expected to show a reasonably smooth continuity without abrupt changes of slopes. Yet, because it is quite difficult in Fig. 25 to connect the boundaries of the left and center B fields without some unusual changes of slopes, a calculation error is suspected. The thermodynamic model reported by [84Kau] is summarized in Table 10.

As expected, the Co-Be phase diagram of Fig. 25 cannot be reproduced at all by this model. A little testing has shown that the left-hand side (2 at.% Be) of the diagram may be calculated using

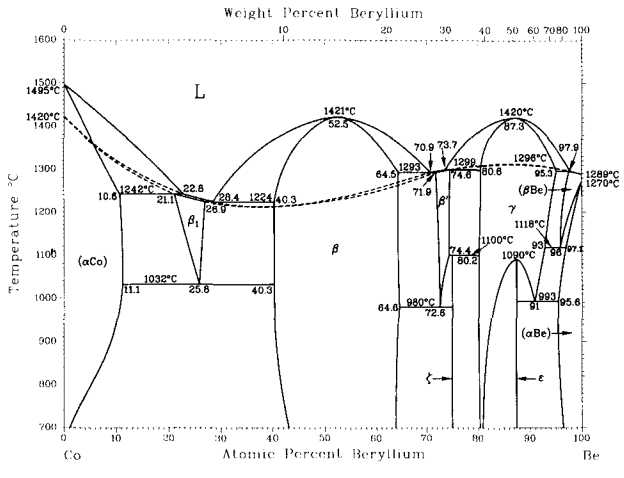

Fig. 26 Calculated Co-Be phase diagram [87Oka3].

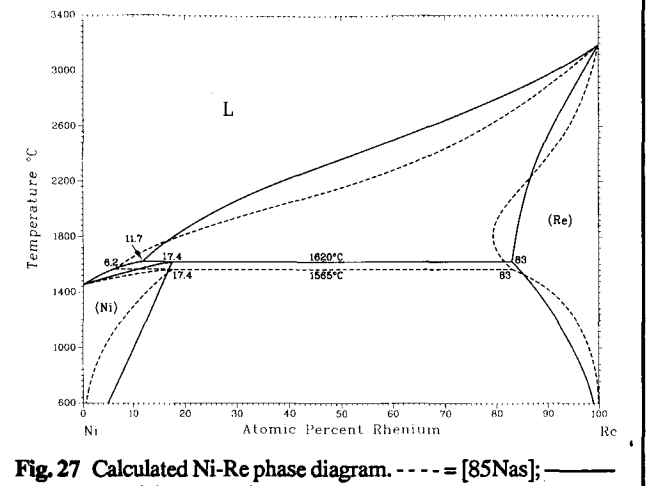

Fig. 27 Calculated Ni-Re phase diagram. - - - - = [85Nas]; ——— = Present model (Table 12).

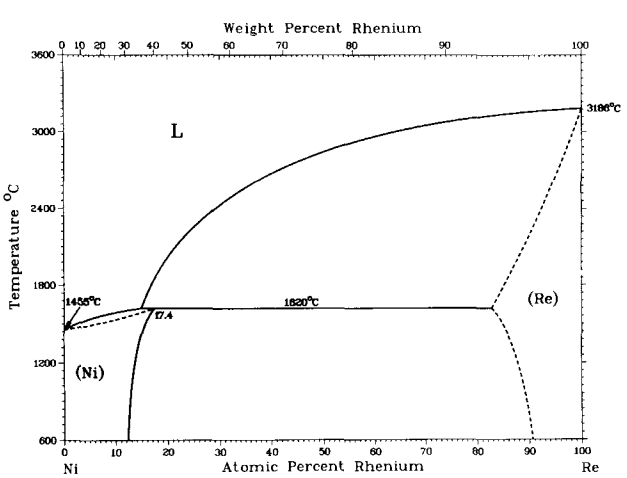

Fig. 28 Assessed Ni-Re phase diagram [85Nas].

the thermodynamic functions of [84Kau] with some reversed signs as given in Table 11.

However, the right-hand side (>50 at.% Be) still remains unaccounted for. Here, the correct thermodynamic model could not be guessed from the phase diagram, or the proposed model. On the other hand, the thermodynamic model proposed by [87Oka3] (Table 12) improves the situation and also makes the liquidus and solidus of the bcc phase smoothly continuous in the metastable range. Maximum and minimum melting points are indicated in the liquidus and solidus trends (Fig. 26).

7.6 Unusual Retrograde Solid Solubility

Dashed lines in Fig. 27 show the Ni-Re phase diagram calculated by [85Nas], which agrees poorly with the assessed experimental phase diagram (Fig. 28). In particular, the retrograde solubility of the (Re) phase in the calculated diagram is very striking. No other

Table 13 Ni-Re Thermodynamic Parameters

Excess Gibbs energy of mixing, J/mol

$\Delta_{mix}G^{ex}(L) = X(1-X)(95\,700-35.3T)$

$\Delta_{mix}G^{ex}(fcc) = X(1-X)(39\,500-4.4T)$

$\Delta_{mix}G^{ex}(cph) = X(1-X)(63\,500-17.5T)$

Lattice stability parameter, J/mol

$G^0(Ni,fcc) = -17\,486.2 + 10.12T$

$G^0(Ni,cph) = -16\,440.2 + 11.464T$

$G^0(Re,fcc) = -27\,830 + 9.62T$

$G^0(Re,cph) = -28\,876.5 + 8.363T$

From [85Nas].

experimental binary phase diagram in [90Mas] shows such a strong retrograde tendency except when ferromagnetic phases are involved. Therefore, the thermodynamic model of [85Nas] (Table 13) was reexamined.

The above expressions, clearly show that the prominent retrograde trend is brought about by the large entropy terms proposed for the liquid and cph phases; that is, both phases are proposed to be well miscible at high temperatures (above approximately the peritectic temperature) and are projected to develop limited solubility at low temperatures. The transition from one tendency to the other brings about the retrograde solubility.

An attempt was made to see how closely the assessed Ni-Re phase diagram (Fig. 28) could be modeled using simpler expressions for the thermodynamic functions. The excess entropies of mixing of the L, fcc, and cph phases were assumed to be zero (see section 4.4). It was found that, even assuming that the L and cph phases are regular solutions, a simpler model given in Table 14 reproduces the assessed diagram much better. The lattice stability parameters are the same as in Table 13. The calculated phase

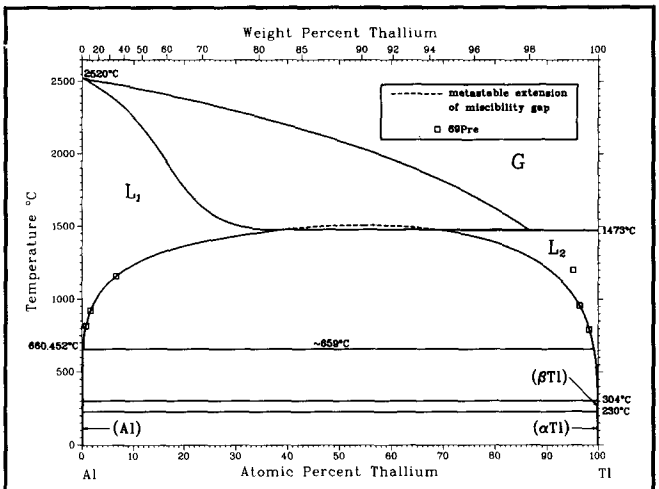

Fig. 29 Assessed Al-Tl phase diagram [89Mca].

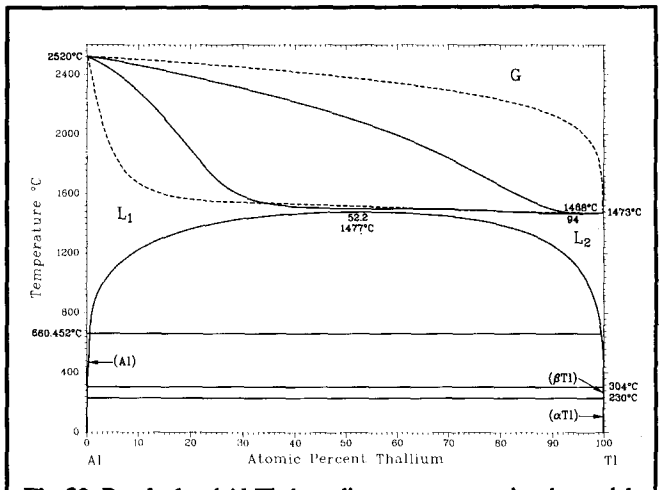

Fig. 30 Recalculated Al-Tl phase diagram. —— = using the model given by [89Mca]; - - - - = using corrected lattice stability

Table 14 Revised Ni-Re Thermodynamic Parameters

Excess Gibbs energy of mixing, J/mol

$\Delta_{mix}G^{ex}(L) = X(1-X)(24\,000)$

$\Delta_{mix}G^{ex}(fcc) = X(1-X)(17\,750 + 41\,845X)$

$\Delta_{mix}G^{ex}(cph) = X(1-X)(30\,500)$

Table 15 Al-Tl Thermodynamic Parameters

Excess Gibbs energy of mixing, J/mol

$\Delta_{mix}G^{ex}(G) = 0$

$\Delta_{mix}G^{ex}(L) = X(1-X)[74\,715.8 - 13\,937X - (26.567 - 8.9266X)T]$

Lattice stability parameter, J/mol

$G^0(Al,G) = 70\,129 - 25.109T$

$G^0(Tl,G) = 39\,215 - 22.460T$

From [89Mca].

diagram is shown in Fig. 27 with solid lines. The unusual retrograde solubility of (Re) is no longer observed.

7.7 Phase Boundaries Crossing One Another

The Al-Tl phase diagram shown in Fig. 29 was calculated by [89Mca] using the thermodynamic model given in Table 15.

When the G/(G+L_1) and (G+L_1)/L_1 boundaries are extrapolated to lower temperatures, these boundaries appear to cross one another, although the existence of a miscibility gap in the liquid state complicates the observation of these trends. In the present reexamination, the Al-Tl phase diagram was recalculated using exactly the same thermodynamic parameters as [89Mca]. The result (solid lines in Fig. 30) indicates that the critical point of the miscibility gap of the liquid exists below the boiling curve, and that the (G+L_1)/L_1 and (G+L_2)/L_2 boundaries are continuous. Accordingly, the unusual situation between two phase boundaries does not exist. It is unclear how Fig. 29 was derived. The present recalculation indicates an azeotropic reaction occurring at 94 at.% Tl and 1468 °C, which is unknown in other metallic systems.

7.8 Small Opening Angle of G + L Two-Phase Field

The Al-Tl phase diagram (Fig. 29) involves another problem, *i.e.*, the initial opening angle of the G + L_1 two-phase field at 0 at.% Tl appears to be too small according to one of the criteria in [91Oka]. As the second step in the reevaluation, the values of the lattice stability parameters in Table 15 were checked against the original reference ([73Hul2]). Apparently, [89Mca] used the heat of vaporization of Al and Tl given in cal/mol in [73Hul2] as J/mol. Hence, a multiplication factor of 4.184 must be used to obtain the appropriate lattice stability parameters of the gas phases of Al and Tl in J/mol, *i.e.*,

$G^0(Al,G) = 293\,420 - 105.06T$

$G^0(Tl,G) = 164\,076 - 93.97T$

The gas-liquid equilibrium of the Al-Tl system using these lattice parameters is shown in the dashed lines in Fig. 30. The boundaries now appear quite normal.

7.9 Two Inflection Points Closely Located to One Another

[91Oka] pointed out that it is unlikely that two inflection points (where the second derivative is zero) should occur along a phase boundary within a close distance to one another. Interestingly, both the liquidus and solidus of the V-Cr phase diagram [82Smi] show two such inflection points within ~30 to 40 at.% Cr (Fig. 31). Again, a look at the thermodynamic model from which this unusual phase diagram was derived seemed worthwhile.

The thermodynamic parameters used by [82Smi] are given in Table 16.

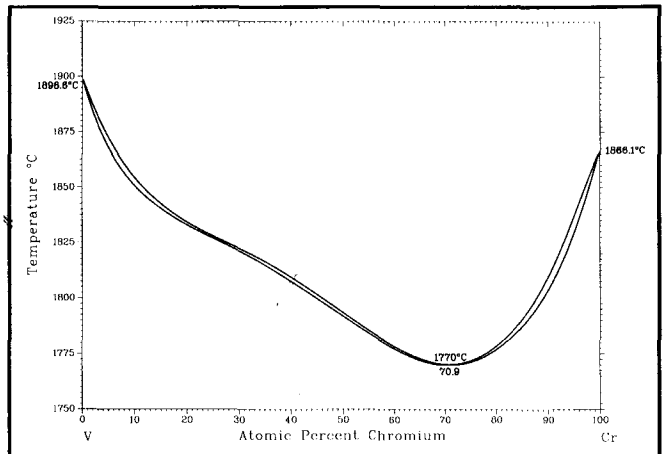

Fig. 31 Assessed V-Cr phase diagram [82Smi]. Recalculated using the thermodynamic parameters given by [82Smi]. Melting points of pure elements are in disagreement with accepted values.

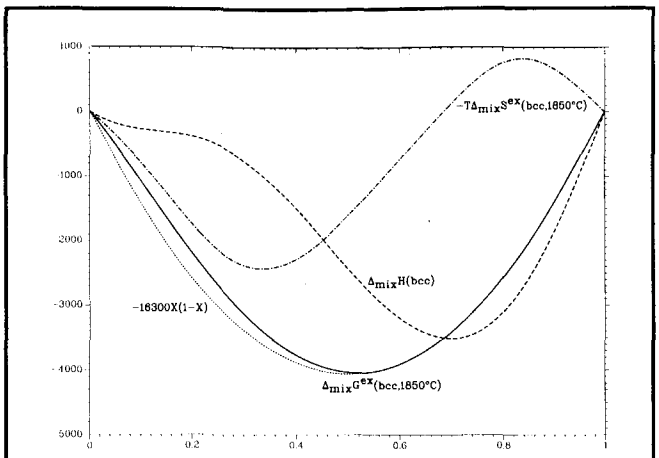

Fig. 32 Thermodynamic functions of bcc (V,Cr), adopted by [82Smi].

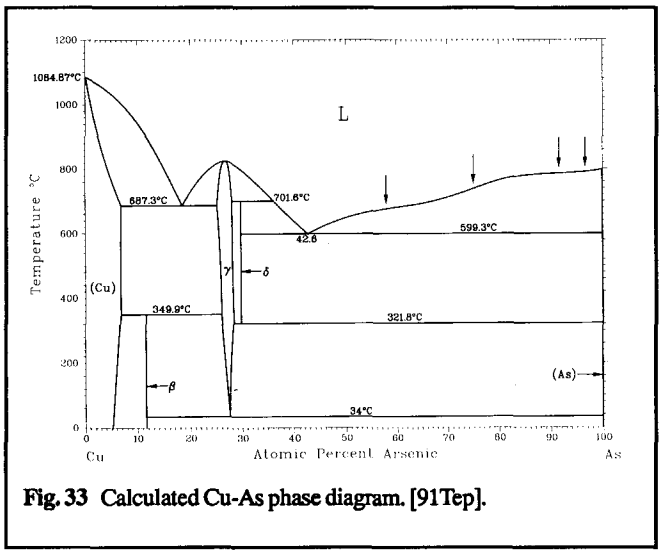

Fig. 33 Calculated Cu-As phase diagram. [91Tep].

Table 16 V-Cr Thermodynamic Parameters

Excess Gibbs energy of mixing, J/mol

$\Delta_{mix}G^{ex}(L) = X(1-X)(-15\,652-7196X)$

$\Delta_{mix}G^{ex}(bcc) = X(1-X)(-6044+43\,856X-145\,096X^2 + 86\,400X^3 - T(1.427+34.910X-87.904X^2+49.504X^3))$

Lattice stability parameter, J/mol

$G^0(V,bcc) = -21\,500-9.9T$

$G^0(Cr,bcc) = -16\,900-7.9T$

From [82Smi].

Table 17 Cu-As Thermodynamic Parameters, [91Tep]

$G^0(As) = -24\,443+22.425T$ J/mol

$\Delta_{mix}G^{ex}(L) = X(1-X)[-46282-17\,660X+572\,387X^2-83\,5306X^3 + 405\,962X^4-(3.0414+70.1086X)T]$ J/mol

[82Smi] obtained the excess Gibbs energy function of the bcc phase by a polynomial fitting of vapor pressure data obtained at 1177 to 1377 °C by [64Ald]. It is difficult to visualize the trend of this complex function. At a glance, this formulation, when compared with the expression for the excess Gibbs energy of mixing of the liquid phase, gives an unusually contrasting impression, because the narrow L + (V,Cr) two-phase field requires that the Gibbs energies of the liquid and the solid phases have similar shapes. If the shapes are quite different, the compositions of the common tangent line to the Gibbs energy curves of the liquid and solid phases would not be able to remain closely located with respect to one another at all temperatures. Also, conceptually, the existence of a minimum melting point means that the solid phase behaves more ideally than the liquid phase (when the excess Gibbs energy of mixing is negative), in contrast to the model of [82Smi]. Figure 32 shows the enthalpy, excess entropy, and excess Gibbs energy of mixing of the bcc phase at 1850 °C, which illustrates how the existence of a narrow two-phase field could be maintained. Although the $\Delta_{mix}H$ and $-T\Delta_{mix}S^{ex}$ functions are strongly composition dependent (see the difference in the partial molar quantities at infinitely dilute solution of (V) and (Cr)), the unusual parts cancel each other and the $\Delta_{mix}G^{ex}$(bcc) function behaves almost like a regular solution. (This "unlikely" behavior was pointed out by [64Ald].) For comparison, a regular solution curve, $\Delta_{mix}G^{ex}(bcc) = -16\,300X(1-X)$ J/mol has been included with a dotted line in Fig. 32. The deviation from this curve is small at >50 at.% Cr and discernible only at 0 to >50 at.% Cr. This deviation from the regular solution curve causes the occurrence of two inflection points. Now, however, because the deviation results from a difference in the strongly composition-dependent enthalpy and excess entropy terms, and the extrapolation is substantial (~500 °C), the formation of two closely-located inflection points can be easily regarded as artificial. Most likely, the separa-

tion of the Gibbs energy into enthalpy and entropy terms was influenced too much by the experimental data of [64Ald].

As the next step, an attempt was made to calculate the liquidus and solidus curves using a subregular solution model (two parameters) for both liquid and solid phases with the same minimum melting point (70.9 at.% Cr, 1770 °C) as [82Smi]. However, an appropriate model was impossible to assemble because the minimum melting point is too far on the Cr side or too low, relative to the small difference in the melting points of V and Cr. Because the melting points of pure V and Cr have not been well defined, the observed decrease in the minimum melting point with respect to the currently accepted melting points of pure elements may have been overestimated. More recently, [85Koc] reported that there is no minimum melting point in the V-Cr phase diagram, which is therefore thermodynamically more plausible.

The Cu-As phase diagram calculated by [91Tep] (Fig. 33) provides another example of an unlikely phase boundary with multiple inflection points. In this case, there are four inflection points on the (As) liquidus (arrows added in Fig. 33). Table 17 shows the thermodynamic parameters used by [91Tep] (originally given as a Redlich-Kister expression).

According to the expression, $\Delta_{mix}G^{ex}(L)$, the partial molar enthalpy of mixing is approximately –46 and +79 kJ/mol at $X = 0$ and $X = 1$, respectively, whereas the values estimated by [83Nie] are –40 and –58 kJ/mol, respectively. The values derived from the model of [91Tep] imply an unlikely situation that the nature of the interaction between As and Cu atoms varies drastically depending on composition. The large positive partial molar quantity in the model of [91Tep] is compensated for by an equally large negative contribution from the entropy term (approximately –80 kJ/mol at the melting point of As). Apparently, the four inflection points in the (As) liquidus were caused by the unusual combination of the composition and temperature dependence of the Gibbs energy function of the liquid phase. Probably, this problem could have been spotted more easily had a polynomial expression as in Table 17 been used to describe $\Delta_{mix}G^{ex}(L)$, rather than the Redlich-Kister expression used by [91Tep].

8. Conclusions

A consistent formulation of thermodynamic functions into a thermodynamic model is increasingly accepted as a very useful tool for checking the validity of proposed phase boundaries, or for predicting portions or whole phase diagrams of many systems. A good model is also useful for describing metastable equilibria or the temperature and composition ranges where experiments are difficult to conduct. As computer programs become more sophisticated, thermodynamic modeling is performed more often and with ease by numerous investigators. This leads to attempts to adjust or check experimental phase boundary data and sometimes also to supplement such data. Here, however, the validity of the thermodynamic model that has been assembled for this purpose is often insufficiently examined. This article attempts to show some examples of unlikely thermodynamic models and some simple ways of checking such model, without going too deeply into the details of the models themselves. Sometimes, a proposed thermodynamic model seems to involve unnecessarily complex formulations. As shown here, a simpler model is usually equally as good in representing available thermodynamic data and in expressing the phase diagram. Usually, the simpler formulation is also more informative making trivial errors or unlikely values of parameters easier to spot.

It must be stressed here that the primary intention of this article is to provide practical hints for screening unrealistic or unlikely thermodynamic models used for phase diagram calculations. Although simple thermodynamic models are shown often to be more realistic and informative, it does not follow that a simple model will always represent the reality of the thermodynamic nature of a given system. Therefore danger exists, especially when the simple model is applied to a situation where substantial extrapolation is involved. For example, the assumption of $\Delta C_p = 0$ recommended often in this article may not be valid when, *e.g.*, the properties of extremely undercooled liquids are considered. However, even when the information on ΔC_p is available and the information is crucial for proper understanding of the nature of the system, the essence of this article must be still remembered: a simpler model of ΔC_p is probably more informative.

Acknowledgment

This article was written because of the encouragement of Dr. W.W. Scott, Jr., ASM International, and the very helpful comments and suggestions of Prof. T.B. Massalski, Carnegie-Mellon University. The author wishes acknowledge with thanks their contributions.

Cited References

27Kaw: M. Kawakami, "The Heat of Mixing of Metals," *Z. Anorg. Chem., 167,* 345-363 (1927) in German.

28Boz: G. Bozza and C. Sonnino, "The Al-Ca System," *Giorn. Chim. Ind. Appl., 10,* 443-449 (1928).

28Mat: K. Matsuyama, "On the Equilibrium Diagram of the Al-Ca System," Sci. Rep. Tohoku Univ., 17, 783-789 (1928).

45Jaf: R.I. Jaffee, E.M. Smith, and B.W. Gonser, "The Constitution of the Gold-Germanium System," *Trans. Metall. Soc. AIME, 161,* 366-372 (1945).

45Owe: E.A. Owen and E.A.O. Roberts, "The Solubility of Certain Metals in Gold," *J. Inst. Met., 71,* 213-254 (1945).

48Kau: W. Kauzmann, "The Nature of the Glassy State and the Behavior of Liquids at Low Temperatures," *Chem. Rev., 43,* 219-256 (1948).

49Kle: O.J. Kleppa, "Thermodynamic Study of Liquid Metallic Solutions. I. The System Lead-Gold," *J. Am. Chem. Soc., 71*(10), 3275-3280 (1949)

55Kle: O.J. Kleppa, "A Thermodynamic Study of Liquid Metallic Solutions. VI. Calorimetric Investigations of the system Bi-Pb, Cd-Pb, Cd-Sn, and Sn-Zn," *J. Phys. Chem., 59,* 354-361 (1955).

56Edw: R.K. Edwards and M.B. Brodsky, "The Thermodynamics of the Liquid Solutions in the Triad Cu-Ag-Au. II. The Cu-Au System," *J. Am. Chem. Soc., 78*(7), 2983-2989 (1956).

56Kle: O.J. Kleppa, "The Thermodynamic Properties of the Moderately Dilute Liquid Solutions of Copper, Silver, and Gold in Thallium, Lead, and Bismuth," *J. Phys. Chem., 60,* 446-452 (1956).

56Oel: W. Oelsen, E. Shumann, H.J. Weight, and O. Oelsen, "On the Thermodynamic Analysis. IV. Calorimetric Measurements of Cd-Pb Liquid Alloys," *Arch. Eisenhuttenwes., 27*(8), 487-511 (1956) in German.

56Ori: R.A. Oriani, "Thermodynamics of Liquid Ag-Au and Au-Cu Alloys and the Question of Strain Energy in Solid Solutions," *Acta Metall., 4*(1), 15-25 (1956).

56Rhi: F.N. Rhines, *Phase Diagrams in Metallurgy*, McGraw Hill Publishing Co., New York, 340 p (1956).

59Mul: K. Muller and W. Merl, "Investigation of Some Noble Metal Alloys Applied in Semiconductor Techniques," *Elektrotech. Z., A, 80*(15), 515-518 (1959) in German.

62Pal: P.E. Palmer, O.D. McMasters, and W.L. Larsen, "Thorium-Vanadium Phase Diagram," *Trans. ASM, 55*, 301-306 (1962).

64Ald: A.T. Aldred and K.M. Myles, "Thermodynamic Properties of Solid Vanadium-Chromium Alloys," *Trans. Metall. AIME, 230*(6), 736-740 (1964).

65Ter: V.F. Terekhova, E.V. Maslova, and Ye.M. Savitskiy, "Iron-Neodymium Equilibrium Diagram," *Izv. Akad. Nauk SSSR, Met.*, (3), 128-130 (1965) in Russian; TR: *Russ. Metall.*, (3), 50-52 (1965).

67Sve: V.N. Svechnikov, A.K. Shurin, and G.P. Dmitriyeva, "The Hafnium-Nickel Equilibrium Diagram," *Izv. Akad. Nauk SSSR, Met.*, (6), 176-179 (1967) in Russian; TR: *Russ. Metall.*, (6), 95-96 (1967).

68Gor: P. Gordon, *Principles of Phase Diagrams in Material Systems*, McGraw Hill Publishing Co., New York, 232 p (1968).

69Hag: J.P. Hager and R.A. Walker, "Galvanic Cell Studies Using a Molten Oxide Electrolyte: Part II—Thermodynamic Properties of the Pb-Au System," *Trans. Metall. Soc. AIME, 245*(10), 2307-2312 (1969).

69Nec: A. Neckel and S. Wagner, "Mass Spectrometric Determination of Thermodynamic Activities. I. Gold-Copper System," *Ber. Bunsenges. Phys. Chem., 73*(2), 210-217 (1969) in German.

69Pre: B. Predel and H. Sandig, "Investigation of Thermodynamics of Binary Systems with Extremely Strong Tendency to Demixing," *Z. Metallkd., 60*, 208-214 (1969) in German.

70Hag: J.P. Hager, S.M. Howard, and J.H. Jones, "Thermodynamic Properties of the Copper-Tin and Copper-Gold System by Mass Spectrometry," *Metall. Trans., 1*, 415-422 (1970).

70Kau: L. Kaufman and H. Bernstein, *Computer Calculations of Phase Diagrams*, Academic Press, New York (1970).

71Ita: K. Itagaki and A. Yazawa, "Measurements of Heats of Mixing in Liquid Copper Binary Alloy," *J. Jpn. Inst. Met., 35*(4), 383-389 (1971) in Japanese.

71Sav: E.M. Savitskii, O.P. Naumkin, and Yu.V. Efimov, "V-Sc Phase Diagram," *Izv. Akad. Nauk SSSR, Met.*, (2), 178-179 (1971) in Russian; TR: *Russ. Metall.*, (2), 119 (1971).

73Hul1: R. Hultgren, P.D. Desai, D.T. Hawkins, M. Gleiser, and K.K. Kelley, *Selected Values of the Thermodynamic Properties of Binary Alloys*, American Society for Metals, Metals Park, OH, 1435 p (1973).

73Hul2: R. Hultgren, P.D. Desai, D.T. Hawkins, M. Gleiser, K.K. Kelley, and D.D. Wagman, *Selected Values of the Thermodynamic Properties of the Elements*, American Society for Metals, Metals Park, OH, 636 p (1973).

75Kau: L. Kaufman and H. Nesor, "Calculation of the Nickel-Aluminum-Tungsten, Nickel-Aluminum-Hafnium, and Nickel-Chromium-Hafnium Systems," *Can. Metall. Q., 14*(3), 221-232 (1975).

75Pre: B. Predel and H. Bankstahl, "Thermodynamic Properties of Liquid Silver-Germanium, Silver-Silicon, Gold-Germanium, and Gold-Silicon Alloys," *J. Less-Common Met., 43*(1-2), 191-203 (1975).

76Kam: K. Kameda, S. Sakairi, and Y. Yoshida, "Activities of Thallium and Lead in Liquid Gold Base Binary Alloys Systems," *J. Jpn. Inst. Met., 40*(4), 387-392 (1976) in Japanese.

77Bar: I. Barin, O. Knacke, and O. Kubaschewski, *Thermochemical Properties of Inorganic Substances (Supplement)*, Springer-Verlag, New York (1977).

77Ber: C. Bergman and R. Castanet, "Thermodynamic Investigation on the Au-Te Binary System," *Ber. Bunsenges., 81*(10), 1000-1003 (1977).

77Leg: B. Legendre and C. Souleau, "The Ternary System Gold-Germanium-Tellurium. Contribution to the Study of Binary Systems Ge-Te and Au-Ge," *J. Chem. Res. S, 12*, 306-307 (1977) in French.

77Luk: H.L. Lukas, E.T. Henig, and B. Zimmerman, "Optimization of Phase Diagrams by a Least Squares Method Using Simultaneously Different Types of Data," *Calphad, 1*(3), 225-236 (1977).

80Mie: A.R. Miedema, P.F. de Chatel, and F.R. de Boer, "Cohesion in Alloys—Fundamentals of a Semi-Empirical Method," *Physica B, 100*, 1-28 (1980).

82Eva: D.S. Evans and A. Prince, "The Au-Pb Phase Diagram," *Alloy Phase Diagrams*, Proc. MRS Meeting, Boston (1982), L.H. Bennett, T.B. Massalski, and B.C. Giessen, Ed., Elsevier North-Holland, Inc., New York (1983).

82Pel: A.D. Pelton, W.T. Thompson, and C.W. Bale, *F*A*C*T (Facility for the Analysis of Chemical Thermodynamics)*, McGill University, Montreal, Quebec (1982).

82Smi: J.F. Smith, D.M. Bailey, and O.N. Carlson, "The Cr-V (Chromium-Vanadium) System," *Bull. Alloy Phase Diagrams, 2*(4), 469-473 (1982).

83Cha: M.W. Chase, "Heats of Transition of the Elements," *Bull. Alloy Phase Diagrams, 4*(1), 123-124 (1983).

83Nie: A.K. Niessen, F.R. de Boer, R. Boom, P.F. de Chatel, W.C.M. Mattens, and A.R. Miedema, "Model Predictions for the Enthalpy of Formation of Metal Alloys. II," *Calphad, 7*(1), 51-70 (1983).

84Kau: L. Kaufman and L.E. Tanner, "Coupled Phase Diagrams and Thermochemical Descriptions of the Iron-Beryllium, Cobalt-Beryllium, Nickel-Beryllium, and Copper-Beryllium Systems," *Calphad, 8*(2), 121-133 (1984).

84Nay: A.A. Nayeb-Hashemi and J.B. Clark, "The Mg-Sn (Magnesium-Tin) System," *Bull. Alloy Phase Diagrams, 5*(5), 466-476 (1984).

84Oka1: H. Okamoto and T.B. Massalski, "The Au-Te (Gold-Tellurium) System," *Bull. Alloy Phase Diagrams, 5*(2), 172-177 (1984).

84Oka2: H. Okamoto and T.B. Massalski, "The Au-Pb (Gold-Lead) System," *Bull. Alloy Phase Diagrams, 5*(3), 276-284 (1984).

84Oka3: H. Okamoto and T.B. Massalski, "The Au-Ge (Gold-Germanium) System," *Bull. Alloy Phase Diagrams, 5*(6), 601-610 (1984).

84Top: L. Topor and O.J. Kleppa, "Thermochemistry of Binary Liquid Gold Alloys," *Metall. Trans. A, 15*, 203-208 (1984).

85Koc: Yu.A. Kocherzhinsky, V.I. Vasilenko, and O.G. Kulik, "Construction of the Melting Diagrams of Some Mo-Containing Systems and the Metastable Melting Diagram of the Cr-C System Using DTA-Technique up to 3000 K," *Thermochim. Acta, 93*, 649-652 (1985).

85Nas: A. Nash and P. Nash, "Ni-Re (Nickel-Rhenium) System," *Bull. Alloy Phase Diagrams, 6*(4), 348-350 (1985).

85Smi: J.F. Smith, K.J. Lee, and D.E. Peterson, "The Th-V (Thorium-Vanadium) System," *Bull. Alloy Phase Diagrams, 6*(4), 369-372 (1985).

86Kar: I. Karakaya and W.T. Thompson, "The Ag-Ir (Silver-Iridium) System," *Bull. Alloy Phase Diagrams, 7*(4), 359-360 (1986).

86Sau: N. Saunders and A.P. Miodownik, "Thermodynamic Aspects of Amorphous Phase Formation," *J. Mater. Res., 1*(1), 38-46 (1986).

86Ver: J.D. Verhoeven, F.A. Schmidt, E.D. Gibson, and W.A. Spitzig, "Copper-Refractory Metal Alloys," *J. Met., 38*(9), 20-24 (1986).

87Oka1: H. Okamoto, D.J. Chakrabarti, D.E. Laughlin, and T.B. Massalski, "The Au-Cu (Gold-Copper) System," *Bull. Alloy Phase Diagrams, 8*(5), 454-474 (1987).

87Oka2: H. Okamoto and T.B. Massalski, "Thermodynamic Modeling," *Phase Diagrams of Binary Gold Alloys,* ASM International, Metals Park, OH, p. V-XIII (1987)

87Oka3: H. Okamoto, L.E. Tanner, and T. Nishizawa, "The Be-Co (Beryllium-Cobalt) System," *Phase Diagrams of Binary Beryllium Alloys,* ASM International, Metals Park, OH, 45-55 (1987).

87Sch: G. Schneider, E.T. Henig, G. Petzow, and H.H. Stadelmaier, "The Binary System Iron-Neodymium," *Z. Metallkd., 78*(10), 694-696 (1987).

88Bor: R. Bormann, F. Gartner, and K. Zoltzer, "Application of the Calphad Method for the Prediction of Amorphous Phase Formation," *J. Less-Common Met., 145,* 19-29 (1988).

88Dut: J. Dutkiewicz, Z. Moser, and W. Zakulski, "The Cd-Pb (Cadmium-Lead) System," *Bull. Alloy Phase Diagrams, 9*(6), 694-701 (1988).

88Fec: H.J. Fecht and W.L. Johnson, "Entropy and Enthalpy Catastrophe as a Stability Limit for Crystalline Material," *Nature, 334,* 50-51 (1988).

88Gre: A.L. Greer, "The Thermodynamics of Inverse Melting," *J. Less-Common Met., 140,* 327-334 (1988).

88Itk: V.P. Itkin, C.B. Alcock, P.J. van Ekeren, and H.A.J. Oonk, "The Al-Ca (Aluminum-Calcium) System," *Bull. Alloy Phase Diagrams, 9*(6), 652-657 (1988).

88Sub: P.R. Subramanian and D.E. Laughlin, "The Cu-Hf (Copper-Hafnium) System," *Bull. Alloy Phase Diagrams, 9*(1), 51-56 (1988).

89Mca: A.J. McAlister, "The Al-Tl (Aluminum-Thallium) System," *Bull. Alloy Phase Diagrams, 10*(2), 112-114 (1989).

89Pam: K. Pamps, K. Dyrbye, B. Torp, and R. Bormann, "Metastable Phase Formation by Ion Mixing of Nb-Al Multilayers," *J. Mater. Res., 4*(6), 1385-1392 (1989).

89She: R.I. Sheldon and D.E. Peterson, "The U-Zr (Uranium-Zirconium) System," *Bull. Alloy Phase Diagrams, 10*(2), 165-171 (1989).

89Smi: J.F. Smith and K.J. Lee, "Sc-V (Scandium-Vanadium)," *Phase Diagram of Binary Vanadium Alloys,* ASM International, Materials Park, OH, 254-256 (1989).

89Sub: P.R. Subramanian and D.E. Laughlin, "The Cu-Ta (Copper-Tantalum) System," *Bull. Alloy Phase Diagrams, 10*(6), 652-655 (1989).

90Mas: T.B. Massalski, H. Okamoto, P.R. Subramanian, and L. Kacprzak, *Binary Alloy Phase Diagrams,* 2nd edition, ASM International, Materials Park, OH, 3542 p (1990)

90Tan: T. Tanaka, N.A. Gokcen, and Z. Morita, "Relationship between Enthalpy of Mixing and Excess Entropy in Liquid Binary Alloys," *Z. Metallkd., 81*(1), 49-54 (1990).

90Tep: O. Teppo, J. Niemela, and P. Taskinen, "An Assessment of the Thermodynamic Properties and Phase Diagram of the System Bi-Cu," *Thermochim. Acta, 173,* 137-150 (1990).

90Zen: K.J. Zeng and Z.P. Jin, "Optimization and Calculation of the Hf-Ni Phase Diagram," *J. Less-Common Met., 166,* 21-27 (1990).

90Zha: W. Zhang, G. Liu, and K. Han, "Fe-Nd (Iron-Neodymium)," in [90Mas], 1732-1735 (1990).

91Fec: H.J. Fecht, "Metastable Phase Formation in Undercooled Liquid Lead Alloys," *Z. Metallkd., 82*(3), 186-191 (1991).

91Oga: T. Ogawa and T. Iwai, "Thermochemical Modelling of U-Zr Alloys," *J. Less-Common Met., 170,* 101-108 (1991).

91Oka: H. Okamoto and T.B. Massalski, "Thermodynamically Improbable Phase Diagrams," *J. Phase Equilibria, 12*(2), 148-168 (1991).

91Tep: O. Teppo and P. Taskinen, "Assessment of the Thermodynamic Properties of Arsenic-Copper Alloys," *Scand. J. Metall., 20,* 141-148 (1991).

92Oka: H. Okamoto, "Review of Fe-RE (Iron-Rare Earth) Systems," to be published in *Phase Diagrams of Binary Iron Alloys,* H. Okamoto, Ed, ASM International, Materials Park, OH (1992).